SAPIENZA
UNIVERSITÀ DI ROMA

Arrhythmia detection and classification through the analysis of human ECG signal

Dipartimento di Informatica, Automazione e Gestionale

Corso di Laurea Magistrale in Master of Science in Engineering in Computer Science

Candidate

Fabrizio Tropeano

ID number 1771734

Thesis Advisor

Prof. Aris Anagnastopoulos

Academic Year 2018/2019

Arrhythmia detection and classification through the analysis of human ECG signal

Master's thesis. Sapienza – University of Rome

This thesis has been typeset by LaTeX and the Sapthesis class.

Version: January 5, 2019

Author's email: tropeanofabrizio@gmail.com

Ringraziamenti

Desidero ringraziare tutte le persone che mi hanno supportato in questi anni di studi universitari, sostenendomi ed accompagnandomi nella realizzazione del mio percorso formativo.

Ci tengo poi a ringraziare il dipartimento di informatica della Sapienza, specialmente nelle persone del mio relatore, il Prof. Aristidis Anagnostopoulos, e del Prof. Ioannis Chatzigiannakis che in questo lavoro hanno avuto un ruolo fondamentale.

Vorrei poi ringraziare i miei amici per essere sempre stati presenti, nei momenti di fatica come nei momenti di soddisfazione, ed avermi aiutato ad affrontare al meglio ogni giornata.

Un sentito grazie va a Giorgia, la mia fidanzata, che è sempre stata per me esempio di professionalità e dedizione al lavoro.

Vorrei inoltre ringraziare le mie nonne per avermi fatto capire ancora di più che la vita è dura ma, per renderla più semplice, va sempre affrontata col sorriso.

Come non ringraziare mio padre e mio fratello per essere sempre stati un saldo punto di riferimento, consigliandomi nelle scelte più difficili e spronandomi a dare il massimo in ogni situazione senza mai farmi sentire la mancanza di qualcosa.

Infine vorrei ringraziare mia madre, credendo che in qualche modo potrà leggere queste parole, per avermi cresciuto con amore ed avermi trasmesso dei sani valori che porterò con me per tutta la vita.

Contents

List of Figures

Chapter 1

Introduction

The *global health organization* estimated that 17.5 million people, around 30% of earth population, died due to cardiovascular diseases so, nowadays, public health assistance has been the object of increasing attention given the exponential growth of the human population and consequently of medical costs. **Arrhythmias** are one of these diseases and they are the consequence of an electrical dysfunction in the cardiac signal of the heart.
There are several approaches to monitor heart parameters but the golden standard is well known as *ElectroCardioGraphy* (ECG), that is the process of recording the electrical activity of the heart. This approach gained a lot of popularity due to the fact that the acquisition of data is not invasive for patients and requires simple and cheap devices. ECG devices are bulky for usage in outside place so, in the last years, wearable mobile devices such as *Wahoo Fitness* and *Polar H10* have been developed.
Arrhythmias can be classified into two major categories [1]. The first category consists of arrhythmias formed by a single irregular heartbeat, herein called *morphological arrhythmias*. The other category consists of arrhythmias formed by a set of irregular heartbeats, herein called *rhythmic arrhythmias*. These heartbeats produce alterations in the morphology or wave frequency, and all of these alterations can be identified by the ECG exam. The process of identifying and classifying arrhythmias can be very troublesome for a human being because sometimes it is necessary to analyze each heartbeat of the ECG records, acquired by a *Holter*[1] monitor for instance, during hours, or even days.
For this reason, automatic arrhythmia detection is crucial in clinical cardiology, especially when performed in real time. Hence, it is easy to guess that an efficient health monitoring system should be able to detect abnormalities of health conditions in a reasonable time maintaining an high accuracy. The function of human body is frequently associated with signals of electrical, chemical or acoustic origin. Extracting useful information from these biomedical signals has been found very helpful in explaining and identifying various pathological conditions. The analysis of arrhythmias starts from the study of each heartbeat composing the ECG. A single pulsation of the heart is represented on the ECG by various waves, namely *P wave*, *QRS Complex* and *T wave*. The heartbeat moment can be located approximately

[1] In medicine, a Holter monitor is a type of ambulatory electrocardiography device, a portable device for cardiac monitoring for at least 24 to 48 hours

on the *R Peak*.
In the last few years, researchers carried out many studies on the analysis and diagnosis of ECG signals in order to detect human heart diseases.
Software QRS detection has been a research topic for more than 40 years [2]. Till now, various methods have been reported by researchers for detection of QRS complexes [3, 4, 5], such as neural networks [6, 7], Hidden Markov Models [8], wavelet transforms [9, 10] and adaptive thresholds [11].
Once R peak locations have been computed, they need to be analyzed in order to detect arrhythmia episodes. Contrary to what was possible to do with heartbeat detection, when we have to detect and classify arrhythmias, there is no easy way to compare algorithms since each method often aims to classify different classes of arrhythmia. Hence, methods are usually based on the detection of a single arrhythmia type and its difference from normal sinus rhythm, or on the discrimination between several kinds of arrhythmia.
A full automatic system for arrhythmia classification from signals acquired by a ECG device can be divided into four steps such as:

1. **ECG signal Preprocessing**
2. **Heartbeat Segmentation**
3. **Feature Extraction**
4. **Classification**

Feature extraction represents the critical part. Many methods have been developed in the time, such as methods based on RR interval extraction [19, 14, 20, 21] or methods based on neural networks [22, 23]. The objective of this thesis is that of managing to detect and recognize arrhythmia episodes through the analysis of human heart's ECG traces. The proposed approach consists of three steps:

1. **Beat Detection:** In order to achieve R peak detection, an algorithm based on adaptive thresholding technique was implemented in *Python* from an available *Matlab* source code [39]. This method starts from the *Pan and Tompkins* approach [12]. The results obtained from this algorithm were then compared to a naive approach called *first-order difference* (FOD), proposed by the package named *PeakUtils* with the method *PeakUtils.peak.indexes*[13].

2. **Beat Classification:** Once we got R peak locations, we had to classify each beat. Hence, we computed RR intervals as unique feature useful for this method and we implemented, again in *Python*, the approach followed by *Tsipouras et al.* [14]. The algorithm is based on a list of rules proposed by experts cardiologists and works on a window of three RR intervals, for a total of four R peaks and classify the third one in four different categories such as Normal Sinus Beats (N), Premature Ventricular Contraction (PVC), Ventricular Fibrillation (VF), 2nd Heart Block (BII).

3. **Arrhythmia Detection and Classification:** Finally, when all the detected beats had been classified, an algorithm, still proposed by *Tsipouras et al.*[14], was implemented in *Python* in order to detect and classify arrhythmia episodes.

The detection and classification is performed using a deterministic automaton that classify sequences of beats into six different categories of arrhythmia such as Ventricular Bigeminy, Ventricular Trigeminy, Ventricular Couplet, Ventricular Tachycardia, Ventricular Fibrillation and 2nd Heart Block. If a sequence of beats will not be labeled into one of these categories, then their rhythm will be assumed to be normal.

1.1 Document Structure

- **Chapter 2:** Introduction to the cardiological field with an explanation of the cardiac cycle
- **Chapter 3:** Description of the methods developed for heartbeat detection
- **Chapter 4:** Explanation of the algorithms developed for arrhythmia detection and classification
- **Chapter 5:** Conclusions and Future work

Chapter 2

Basic Cardiological Principles

[36]The process of recording the electrical activity of the heart over a period of time, using electrodes, is called ElectroCardioGraphy (ECG). The information recorded on the ECG represents the heart's electrical activity. The pattern displayed on the ECG is called **rhythm**. Hence, the word arrhythmia refers to a heart rhythm dysfunction.

2.1 Human Heartbeat

Most of the information contained on the ECG represents the electrical activity of the myocardium. A generic example of ECG is the following:

Figure 2.1. ECG trace example

As can be easily seen, in this excerpt it is possible to identify five beats. Since this is a normal heart rhythm with no abnormal episodes, all heartbeats have more or less the same structure. Going deeper, it is possible to study the heartbeat in its complex form. The next picture describes how a single normal beat appears on a ECG trace, showing the shape of the beat with all its waves.

Figure 2.2. Human heartbeat waves (PQRST)

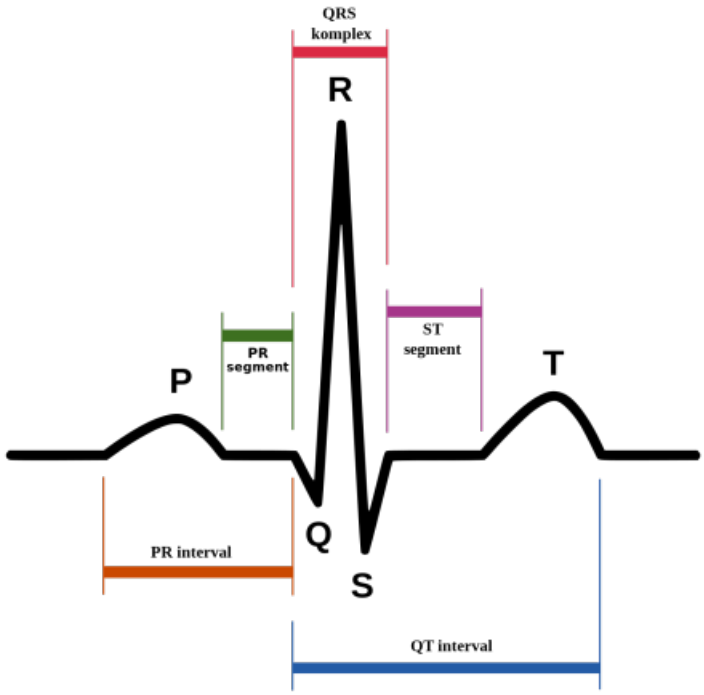

2.1.1 Cardiac Cycle

At the beginning of the cycle, when the heart is in a resting state, positive and negative electrical charges are balanced. This is called the *polarized state* and no electrical flow is generated. When a cell is at rest, it maintains what is known as a resting potential. In the strictest sense, a resting polarized cell has a negatively charged interior and a positively charged outside surface. To maintain this electrical imbalance, microscopic positively and negatively charged particles called *ions* are transported across the cell's plasma membrane. The resting potential must be established within a cell before the cell can be depolarized. After a cell has established a resting potential, that cell has the capacity to undergo depolarization. A difference of potential between the interior of the heart and the outside is needed for the muscle in order to receive the stimulus to start beating. The process of the electrical discharge and flow of electrical activity is called *depolarization*.

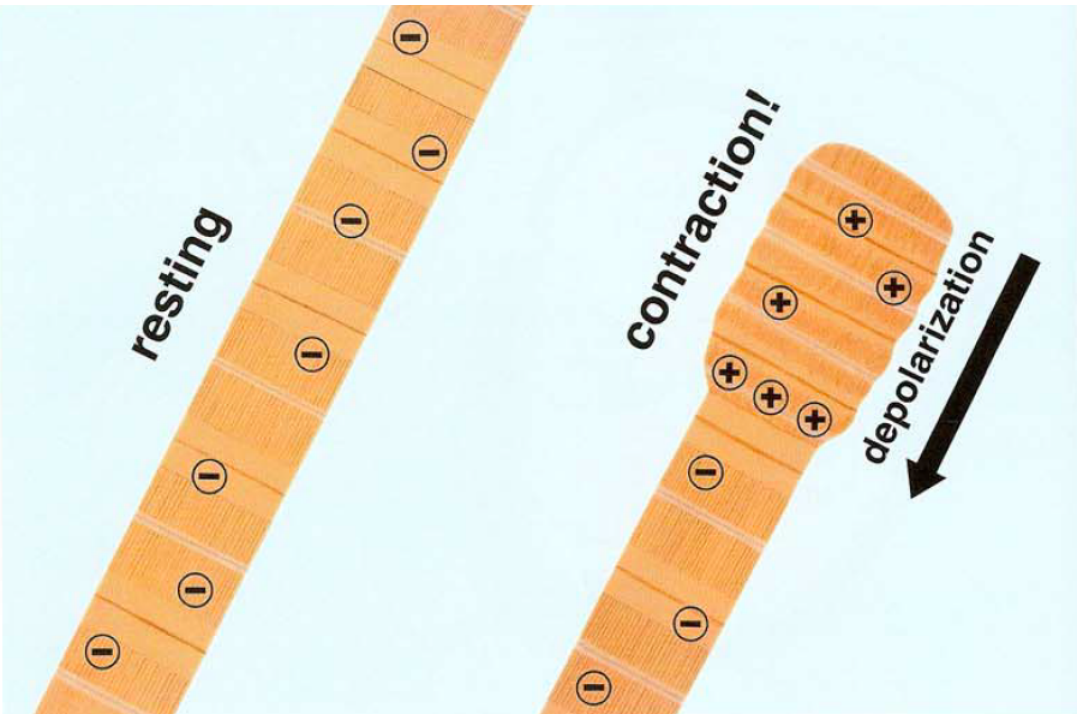

Figure 2.3. Beginning of the depolarization process

During depolarization, the membrane potential rapidly shifts from negative to positive. The process that follows the depolarization, which leads the heart to the initial state, is called *repolarization*. The depolarization, cell interiors turn positive, and repolarization, cell interiors turn negative, are recorded on ECG traces in the following way:

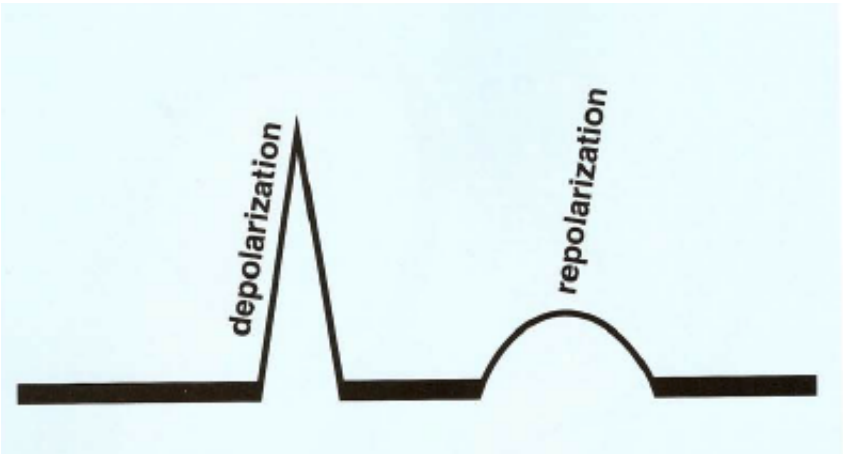

Figure 2.4. Depolarization and Repolarization processes on a ECG trace

Normally, the electrical activity originates in the *SinoAtrial* (SA) *node*. Hence, the SA node is the heart's dominant pacemaker, and its pacing activity is known as

sinus rhythm. The generation of pacemaking stimuli is automaticity. Other focal areas of the heart that have automaticity are called *automaticity foci*.
The SA Node, located in the upper-posterior wall of the right atrium, initiates a depolarization wave at regular intervals to accomplish its pacemaking responsibility. When both atria contract, the blood they contain is forced to pass through the *AtrioVentricular* (AV) *valves* between the atria and the ventricles. The **mitral** and **tricuspid** valves prevent ventricle-to-atrium blood backflow, and they electrically insulate the ventricles from the atria, except for the *AV Node*, that is the only conducting path between the atria and the ventricles.
Oxygen-depleted venous blood enters the right atrium. Atrial contraction forces blood through the tricuspid valve into the right ventricle, which pumps it into the lungs. Oxygenated blood from the lungs enters the left atrium, which contracts to force blood through the mitral valve into the left ventricle. The powerful left ventricle, in turn, pumps blood through the *aorta* to all areas of the body.
Note that, when the electrical activity leaves AV node, the impulses go through the *Bundle of His* to reach the *right* and *left* bundle branches, located within the right and left ventricles. At the terminal ends of the bundle branches, small fibers distribute the electrical impulses to muscle cells to stimulate contraction. These fibers are called *Purkinje fibers*.
The wave of depolarization that flows in the heart is generated by the dominant pacemaker, that is the SA node.

Figure 2.5. Medical point of view of an heart

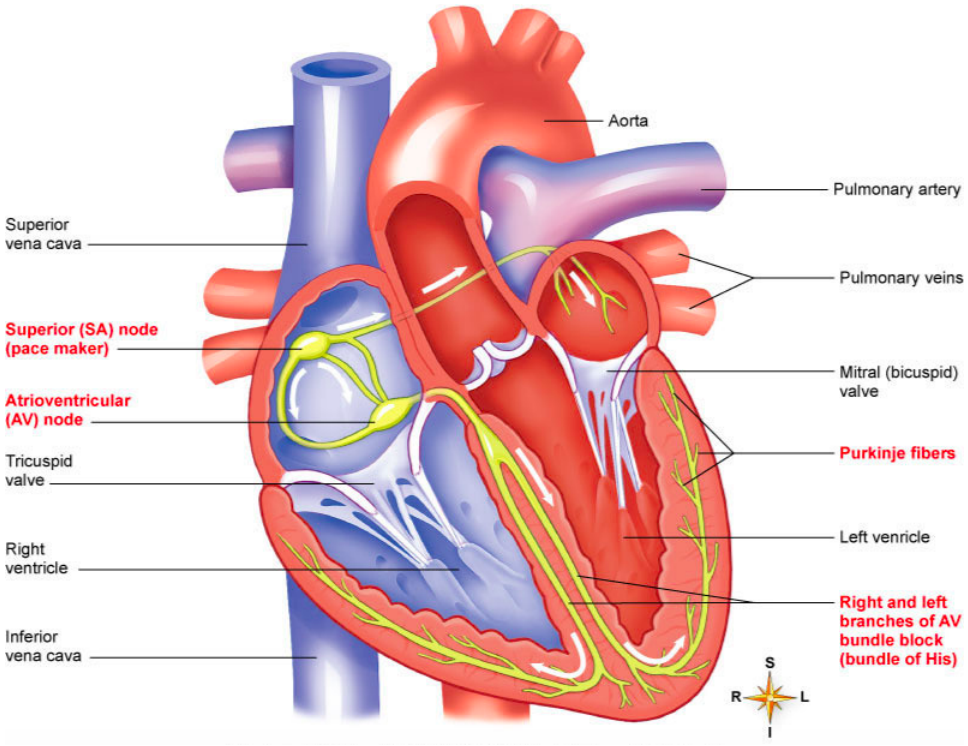

2.1.2 P Wave

The wave of depolarization originated in the SA node stimulates the atria to contract as the wave advances. Each depolarization wave passes through both atria, left and right, producing a *P wave* on the ECG trace. Therefore, the P wave is an upward positive wave generated by an atrial depolarization.

Figure 2.6. P Wave

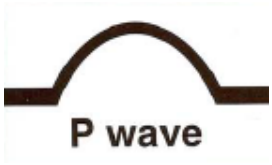

The P wave represents the simultaneous contraction of the atria that forces the blood they contain to pass through the Atrio-Ventricular (AV) node, the only allowed path between atria and ventricles. Note that the blood cannot flow back. When the depolarization wave enters the AV node, a short pause, named *PR Segment*, is produced allowing the blood in the atria to enter the ventricles. A *segment* identifies a straight line or area of electrical inactivity between waves.

Figure 2.7. PR segment produced by the depolarization of the AV node

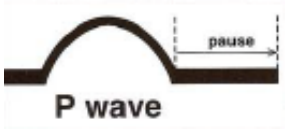

2.1.3 QRS Complex

The QRS complex is a name for the combination of three of the graphical deflections seen on a typical electrocardiogram. It corresponds to the depolarization of the right and left ventricles of the human heart and contraction of the large ventricular muscles. The Q, R and S waves occur in rapid succession, do not all appear in all leads, and reflect a single event and thus are usually considered together. The QRS complex actually represents the beginning of ventricular contraction.

Figure 2.8. QRS Complex

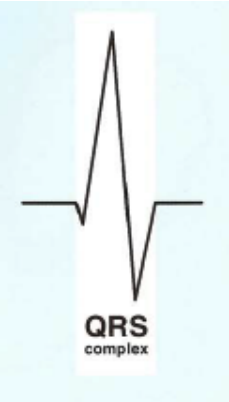

The Q wave is not always present on ECG but, when it is clearly recognizable, it represents the first downward wave of the QRS complex. The Q wave is followed by an upward R wave and after it by a downward S wave. Note that an upward wave is always called an R wave. The distinction between a Q wave and an S wave. that are both downward waves, depends on whether such a downward wave occurs before or after the R wave. In the case an R wave is not clearly detectable we could not say if a downward wave would be a Q wave or an S wave so we would call it a QS wave.

2.1.4 ST Segment

The ST segment is an horizontal baseline segment and it follows the QRS complex. This segment is at the same level of the other baseline segments such as the PR segment. If the ST is elevated or depressed with respect to the normal baseline level, this is usually a sign of serious pathology that may indicate imminent problems, such as myocardial ischemia [15]. The ST segment actually identifies the initial phase of ventricular repolarization.
The T wave is rapid and usually, it is a low but broad wave and represents the end phase of ventricular repolarization. Repolarization occurs so that the ventricular myocytes can recover their interior, resting negative charges, in order to be ready for a new depolarization. The atria repolarize too, but this event is not significant enough to show up on the ECG trace.

Figure 2.9. ST segment and T wave

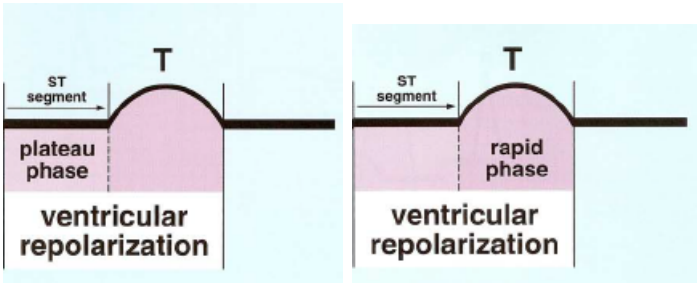

2.1.5 QT Interval

An *interval* refers to the area between waves. Since ventricular systole lasts from the beginning of the QRS until the end of the T wave, the QT interval has clinical significance. Patients with hereditary Long QT interval (LQT) syndromes are vulnerable to dangerous rapid ventricular rhythms. The QT interval, of course, varies with heart rate given that with a rapid heart rate both depolarization and repolarization occur faster.

2.2 Electrocardiogram

The ECG arises because active tissues within the heart generate electrical currents which flow most intensively within the heart muscle itself, and with lesser intensity throughout the body. The flow of current creates voltages between the sites on the body surface where the electrodes are placed. The positioning of an electrode allows seeing a single view of the heart's electrical pattern. Each view of the heart is called *lead*. For sophisticated ECG interpretation, many leads are inspected to visualize the entire heart, however, for basic interpretations of arrhythmia, only one single lead can be considered sufficient. A standard ECG is composed of six limb leads (I, II, III, AVR, AVL, AVF) recorded by using arm and leg electrodes and of six chest leads obtained by placing a suction cup electrode at six different positions on the chest (V1 to V6). To obtain the limb leads, electrodes are placed on the right arm, the left arm and the left leg. A pair of electrodes, one negative and one positive, is used to record a lead. Each bipolar limb lead is recorded using two electrodes so, by selecting a different pair of electrodes for each lead, three separate bipolar limb leads are created, respectively lead I, lead II, lead III.

Figure 2.10. Limb leads I, II, III

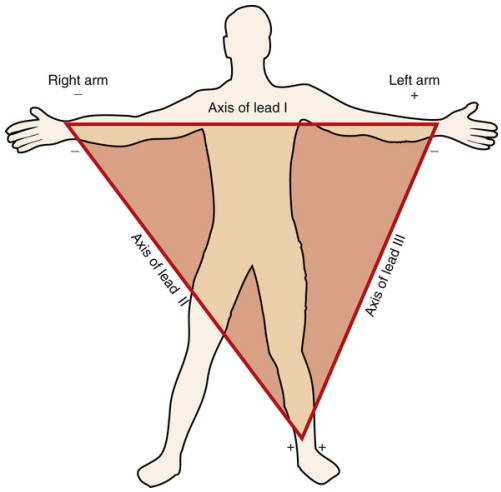

Lead II was the first widely used monitoring lead, but now it is common to use other leads as well, especially variations of the chest leads. A monitoring lead is a single lead that gives good pictures of the basic waves and it is useful to monitor patterns such as arrhythmia.
In long-term monitoring electrode impedance can increase considerably, resulting in very low signal-to-noise ratio, which can make detection practically impossible with a single lead. Therefore, usually two or three leads are used for monitoring [16].
Another standard lead is the Augmented Voltage left Foot (AVF) lead, that uses the left foot electrode as positive and both arm electrodes as a common ground (negative). *Dr. Emanuel Goldberger* designed this new type of lead and he went

on to produce two more leads using the same technique. These two augmented limb leads are called Augmented Voltage Right arm (AVR) and Augmented Voltage Left arm (AVL). For what concern AVR the right arm electrode is positive and the remaining two electrodes are negative while for AVL, the left arm electrode is positive and the other tow electrodes are negative.
The reason to use more than one lead is that it could be hard to see a specific wave in a single given lead, but with six different lead positions, it is more likely to find almost all the relevant waves.
To obtain the six standard chest leads, a positive electrode is placed at six different positions on the chest as you can see in the picture below: To obtain the six standard chest leads, a positive electrode is placed at six different positions on the chest as you can see in the picture below:

Figure 2.11. Chest leads V1 to V6

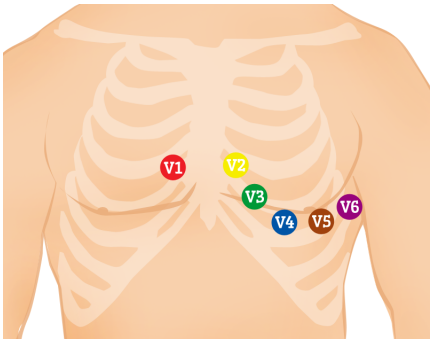

In general, each of the chest leads is oriented through the AV node and projects through the human's back, that is considered to be negative. Moreover, the projection of the heartbeat on ECG is actually different for each single lead, from V1 to V6 as shown below:

Figure 2.12. Heart projection for six different chest leads

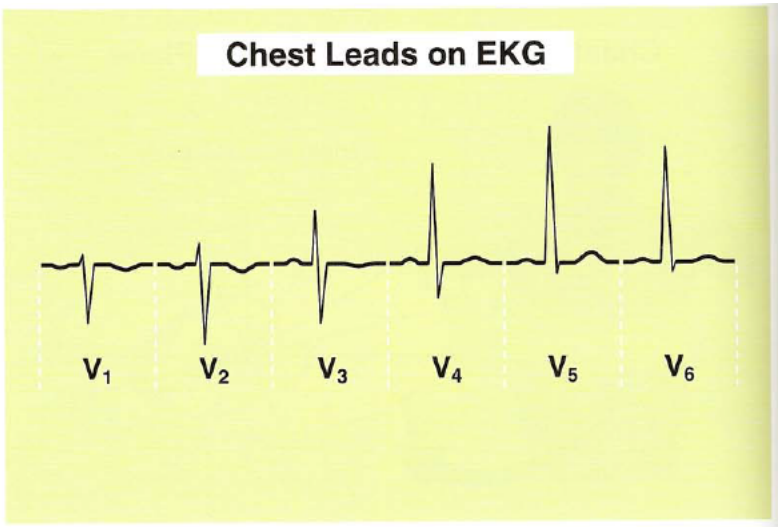

It is easy to see that for V1 projection, the QRS complex is almost totally negative while going on, until reaching V6, the QRS complex get enhanced and becomes mainly positive. This happens because of the position where the electrodes are placed and the projection follows the flow of depolarization wave.
There is a basic rule regarding the flow of electricity through the heart and out of the electrodes: if the electricity flows towards the positive electrode, the patterns produced on the graph paper will be upright. Conversely, if the electricity flows away from the positive electrode or passes through the negative one, the pattern will be a downward deflection.

2.3 The Heart Rhythm

When examining an ECG trace, the first value to determine should be the rate, that is read as cycles per minute. The SA Node, that is the heart's pacemaker and the dominant center of automaticity, generates a *sinus rhythm*. The SA node paces the heart in the normal rate range of 60 to 100 beats per minute. If the SA node paces the heart at a rate slower than 60 beats per minute, this is called *Sinus Bradycardia*. On the other hand, if the SA node paces the heart at a rate greater than 100 beats per minute, this is called *Sinus Tachycardia*.
If normal SA node pacemaking fails, other potential pacemakers known as automaticity foci, also called ectopic foci. They are positioned in the atria, the ventricles and the AV junction and have the following inherent rates:

- **Atrial foci:** 60-80 beats per minute
- **Junctional foci:** 40-60 beats per minute
- **Ventricular foci:** 20-40 beats per minute

Note that, if SA node fails, atrial focus assumes pacing responsibility and if it fails, junctional focus assumes pacing responsibility. Finally, if SA node, atrial focus and junctional focus fail, ventricular focus assumes pacing responsibility. Arrhythmia literally means without rhythm, however it is used to denote any abnormal rhythm. The term arrhythmia actually refers to any change from the normal sequence of electrical impulses. The electrical impulses may happen too fast, too slowly, or irregularly, causing the heart to beat too fast, too slow or irregularly [17].The ECG records the heart's electrical phenomena that may not be seen, felt or heard on physical examination, so the ECG is a very accurate means of recording rhythm disturbances. On ECG there is a consistent distance between similar waves during a normal, regular cardiac rhythm, because the SA Node's automaticity precisely maintains a constant cycle duration between the pacing impulses that it generates. All automaticity foci pace with a regular rhythm. Arrhythmias are broken down into:

- **Slow Heartbeat:** Bradycardia
- **Fast Heartbeat:** Tachycardia
- **Irregular Heartbeat:** Flutter or Fibrillation
- **Early Heartbeat:** Premature Contraction

Any interruption to the electrical impulses that cause the heart to contract can result in arrhythmia. The most common *Arrhythmia* is named *Sinus Arrhythmia* but, even if it sounds pathological, it functions in all humans at all times. This kind of arrhythmia is relatable to the phases of respiration so even if it is called sinus arrhythmia, it is not a true arrhythmia. It is actually considered as a normal, but extremely minimal, increase in heart rate during inspiration, and an extremely minimal decrease in heart rate during expiration. However, arrhythmias can be classified into two macro-categories such as *rhythmic arrhythmias* and *morphological*

arrhythmias. The first category consists of arrhythmias formed by a set of irregular heartbeats while the second category consists of arrhythmias formed by a single irregular heartbeat. [1]

2.3.1 Rhythmic Arrhythmias

Rhythmic arrhythmias can be divided again into a few general categories, according to the arrhythmia's mechanism of origin:

- **Irregular Rhythms:** They are caused by multiple, active automaticity sites. The most common arrhythmia of this category is the *Atrial Fibrillation* that is caused by the continuous rapid-firing of multiple atrial ectopic foci. No single impulse depolarizes the atria completely, and only an occasional, random atrial depolarization reaches the AV node to be conducted to the ventricles, producing an irregular ventricular (QRS) rhythm. Only the occasional atrial impulse gets trough the AV node to initiate a QRS complex. The irregular ventricular response may result in either a slow or rapid ventricular rate, but it is *always* irregular.

- **Escape Rhythms:** The word *escape* describes the response of an automaticity focus to a pause in the pacemaking activity. If SA node pacing ceases entirely, an automaticity focus will escape pacing at its inherent rate, producing an *escape rhythm* that could be atrial, junctional or ventricular. On the other hand, if the pause in pacing is brief, that means that only one cycle is missed, an automaticity focus may escape emitting a single *escape beat* before the normal sinus rhythm returns. We can distinguish three different types of escape beat, that are atrial, junctional and ventricular.

- **Tachy-Arrhythmias:** They originate in a very irritable focus that paces rapidly. Sometimes more than one single active focus is generating pacing stimuli at once. A tachyarrhythmia is easily recognized by rate alone, but the specific diagnosis requires the identification of the origin, that could be in the atrial focus, junctional focus or ventricular focus. The rate changes of the tachyarrhythmia are Paroxysmal Tachycardia (150-250 beats per minute), Flutter (250-350 beats per minute) and Fibrillation (350-450 beats per minute).

2.3.2 Morphological Arrhythmias

Morphological arrhythmias can be recognized by irregularities in the shape of a single beat, observable on the ECG trace. Therefore, in this context, we focus on *arrhythmic beats*. Firstly , it is possible to distinguish between *Escape* beats and *Premature* beats. An *escape* beat is a single beat composing an *escape rhythm* (Subsection 2.3.1).
Premature beats originates in an irritable ectopic focus that fires spontaneously, producing a beat earlier than expected in the rhythm. This kind of beat can be originated by atrial focus, junctional focus or ventricular focus. Premature beats can cause peculiarities in the rhythm that may mimic more serious problems such as pathological conduction blocks. Arrhythmic beats can also be classified into

four sub-categories, according to the *Association for the Advancement of Medical Instrumentation* (AAMI) standard [18], based on the heart location originating the beats:

- **N-class:** This class includes beats originating in the sinus node such as normal and bundle branch block beat types.
- **S-class:** It includes supraventricular ectopic beats.
- **V-class:** Ventricular ectopic beats form this class.
- **F-class:** This class comprises beats that result from fusing normal beats and ventricular ectopic beats.

Furthermore, each class contains more fine-grained classes of arrhythmic beats, that can be view in the table below.

Table 2.1. AAMI Beat Categories Classification

CLASSES	N	S	V	F
DEFINITIONS	Normal Beat	Atrial Premature Beat	Premature Ventricular Contraction	Fusion of Ventricular and Normal Beat
	Left Bundle Branch Block Beat	Aberrated Atrial Premature Beat		
	Right Bundle Branch Block Beat	Nodal (junctional) Premature Beat	Ventricular Escape Beat	
	Atrial Escape Beat	Supraventricular Premature Beat		
	Nodal (junctional) Escape Beat			

2.3.3 Beat Classification

For what concern our purposes, as written in Tsipouras' paper [14], we will classify each beat into four different beat categories, that are :

1. **Normal**
2. **Premature Ventricular Contraction** A premature ventricular beat originates suddenly in an irritable ventricular automaticity focus and produces a giant ventricular complex on ECG. It is a relatively common event where the heartbeat is initiated by Purkinje fibers in the ventrcies rather than by the sinoatrial node, that is the normal heartbeat initiator. PVCs may cause no symptoms at all, but they may also be perceived as a *skipped beat* or felt as palpitations in the chest. Single beat PVC abnormal heart rhythms do not usually pose a danger. Very frequent PVCs are considered a risk factor for arrhythmia-induced cardiomyopathy, in which the heart muscle becomes less effective and symptoms of heart failure may develop. Reading an ECG, they are easy to identify thanks to their great width and enormous amplitude (height and depth). Usually, they are opposite the polarity of the normal QRSs (e.g. if QRS complexes are upwards, PVCs are downwards).

Figure 2.13. Premature Ventricular Contraction Example Trace

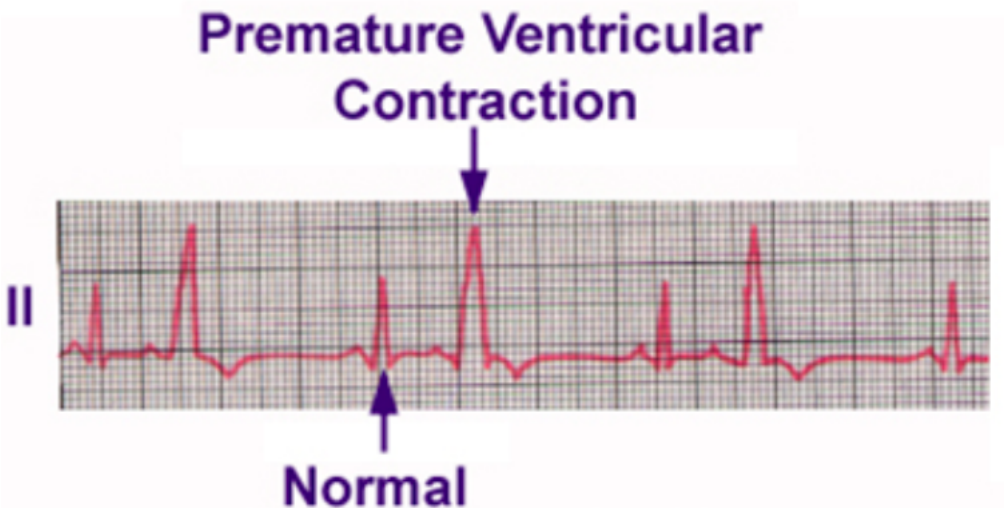

3. **Ventricular Flutter/Fibrillation** This is actually a rhythm annotation. Ventricular fibrillation is caused by rapid-rate discharges from many irritable, parasystolic ventricular automaticity foci, producing an erratic, rapid twitching of the ventricles (ventricular rate is 350-450 beats per minute). This erratic twitching of ventricular fibrillation has been called *bag of worms* since this is the way the ventricles actually appear. On ECG the tracing is totally erratic, without identifiable waves, and the ventricles do not provide mechanical pumping. Hence, ventricular fibrillation is a type of cardiac arrest, for there is no pumping action by the heart.

Figure 2.14. Ventricular Fibrillation Example Trace

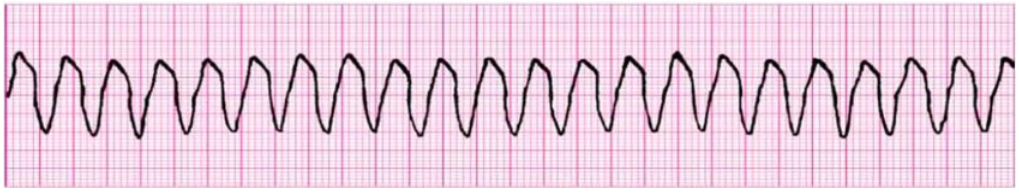

4. **2nd Heart Block** This is actually a rhythm annotation. Second degree AV blocks allow some atrial depolarizations (P waves) to conduct to the ventricles (producing a QRS response), while some atrial depolarizations are blocked, leaving lone P waves without an associated QRS. There are two general types of second degree AV block; those that occur in the AV node (Mobitz I), and those that occur below the AV node (Mobitz II). Mobitz I blocks produce a series of cycles with progressive blocking of AV node conduction until the final P wave is totally blocked in the AV node, eliminating the QRS response.

Figure 2.15. Mobitz I Example Trace

Mobitz II blocks produce a series of cycles consisting of one normal PQRST cycle preceded by a series of paced P waves that fail to conduct through the AV node (no QRS response). It is important to know that Mobitz I type of blocks is considered innocuous while Mobitz II is considered pathological.

Figure 2.16. Mobitz II Example Trace

2.3.4 Arrhythmia Classification

Once we have all beats classified, we classify also arrhythmia episodes. Analyzing beats' sequences, we will find for six arrhythmia categories, that are:

1. **Ventricular Couplet:** The appearance of two consecutive premature ventricular contractions is called ventricular couplet. The PVCs forming the ventricular couplet may have different morphologies.

2. **Ventricular Bigeminy:** Bigeminy is a heart rhythm problem in which there is a continuous alternation of long and short heart beats. Most often this is due to ectopic beats occurring so frequently that there is one after each sinus beat. The two beats are figuratively two twins. The ectopic beat is typically a premature ventricular contraction. For example, in a ventricular bigeminy, a sinus beat is shortly followed by a PVC, a pause, another normal beat, and then another PVC. (e.g. PVC - N - PVC - N - PVC).

3. **Ventricular Trigeminy:** Trigeminy refers to an irregular heartbeat or arrhythmia. Trigeminy may occur randomly or during specific intervals. The condition is more common in older individuals with underlying heart disorders

such as coronary artery disease, mitral valve prolapse and cardiomyopathy. A trigeminy is when there is a repetitive series of two normal heartbeats and one premature ventricular contraction. Very third heartbeat is said to be ectopic. (e.g. PVC - N - N - PVC - N - N - PVC).

4. **Ventricular Tachycardia:** Ventricular tachycardia is a type of regular, fast heart rate that arises from improper electrical activity in the ventricles of the heart. Although a few seconds may not result in problems, longer periods are dangerous. Ventricular tachycardia may result in cardiac arrest and turn into ventricular fibrillation. It can occur due to coronary heart disease, aortic stenosis, cardiomyopathy, electrolyte problems or a heart attack.

5. **Ventricular Flutter/Fibrillation:** Ventricular fibrillation is caused by rapid-rate discharges from many irritable, parasystolic ventricular automaticity foci, producing an erratic, rapid twitching of the ventricles (ventricular rate is 350-450 beats per minute). This erratic twitching of ventricular fibrillation has been called *bag of worms* since this is the way the ventricles actually appear. On ECG the tracing is totally erratic, without identifiable waves, and the ventricles do not provide mechanical pumping. Hence, ventricular fibrillation is a type of cardiac arrest, for there is no pumping action by the heart.

6. **2nd Heart Block:** Second degree AV blocks allow some atrial depolarizations (P waves) to conduct to the ventricles (producing a QRS response), while some atrial depolarizations are blocked, leaving lone P waves without an associated QRS. There are two general types of second degree AV block; those that occur in the AV node (Mobitz I), and those that occur below the AV node (Mobitz II). Mobitz I blocks produce a series of cycles with progressive blocking of AV node conduction until the final P wave is totally blocked in the AV node, eliminating the QRS response.

Chapter 3

Beat Detection

The only tool available to physicians and cardiologists to evaluate irregular heart rate, heart rhythm, and diagnose cardiac abnormalities are Electrocardiography monitoring devices (ECG). Such high-accuracy devices that are capable of recording the heart's patterns are available only in hospitals and are bulky for usage in outside place.
To overcome this problem, in the last few years, wearable devices have been developed such as Wahoo Fitness, Polar H10 Heart Rate Sensor etc. Currently available portable ECG devices rely on 1-3 leads which have limited accuracy and reliability, as electromagnetic noise may be either of environmental (e.g., mobile phones, electrical wires, appliances) or internal origin (e.g., produced by muscular contractions) and remains a frequent source of abnormally appearing ECGs. [24].
This problem is addressed by introducing more than one recording points (three, six, twelve ECG leads) in order to acquire more information from more than one heart regions. However, considering additional recording points increase the power consumption of the device and produce a high-definition signal that requires bigger memory capacity to be stored [25]. This creates a trade-off between accuracy and longevity of the wearable device.
Fog computing is considered as the most promising enhancement of the traditional cloud computing paradigm in order to handle potential issues introduced by the emerging *Internet of Things framework* at the network edge. Fog and edge computing in general is an emerging platform that provides computational, storage, and control resources in an intermediate layer between end-user devices and cloud computing data centers.
Offloading large datasets to the core network is no longer a necessity, consequently leading to improved safety and quality of experience (QoE) [26]. Furthermore, fog computing also resolves a series of IoT-related constraints such as:

- **Extensive bandwidth requirements:** The phenomenal growth of the IoT ecosystem towards supporting billions of devices, generates a data-oriented issue. Lots of barren datasets are collected to by the end nodes and are submitted to the cloud to be processed. Such an approach appears to be rather ineffective, since it consumes hefty amounts of bandwidth before possibly categorizing the processed data as null and meaningless. Hence, a certain level of preprocessing to the edge of the network is rather compulsory. Data

trimming on the edge will effectively reduce bandwidth requirements and consequently traffic costs and necessary cloud storage.

- **Necessity for decreased latency and autonomous operation:** As the total number of interconnected nodes increases, cloud services will encounter severe challenges towards providing uninterrupted services in cases of irregular connectivity. The advent of 5G will most probably solve the majority of connectivity issues currently compromise service continuity in the cloud, but since redundancy and robustness are required in existing deployments, one could consider fog computing as an intermediate or supplementary method of addressing these issues. Obtained sensor data could be temporarily stored, potentially pre-processed in the intermediate layer, from which operators may get notifications regarding ill operation or imminent danger. Cloud connectivity is not a must and latency is decreased since only one logical hop is required for the system to provide a preliminary response.
- **Enhanced Reliability and Security prerequisites:** As more data traverse through the network the possibility of error also increases, since bit error rate, data transmission latency and packet droppings are proportional to the actual size of transmitted data. Such an increased error margin cannot be tolerated when emergency or safety critical applications rely their proper functionality on similar techniques. Uninterrupted service is of paramount importance for IoT applications, together with protecting resource constrained devices, update the security level of large distributed systems in a trustworthy manner and response to compromises without causing intolerable disruptions [27]. Fog enables service cohesion and stability by acting as complementary layer to the cloud and the necessary endpoints.

Fog computing unveils a novel architectural concept that will most likely also enable fascinating business models for computing and networking. The major advantage of fog is no other than supporting networking in the edge, together with all the delay-critical services that can be deployed in this layer.
Healthcare applications are definitely amongst the prime examples of solutions benefited by the efficient monitoring. The heterogeneous nature, the extensive distribution and the hefty number of deployed IoT nodes will disrupt functional models, creating confusion. However, IoT will facilitate the rise of new applications, with automated Healthcare monitoring platforms being amongst them.
An automated healthcare application [28] allows patients to share information to their physicians, monitor their health status independently and notify the authorities rapidly in emergency situations. Any advanced healthcare monitoring system must be used from both patients and doctors, offline or in real-time, and under all circumstances. In general, a comprehensive fog-based healthcare monitoring system should support patient self-monitoring, physician offline monitoring through accessing obtained datasets from various user devices, physician online monitoring and patient monitoring within healthcare infrastructures such as hospitals and day-care centers. This analysis leads to the accurate definition of four use cases:

1. **Patient self-monitoring:** This use case refers to end-users that would like to perform self-monitoring of their medical conditions.

2. **Physician off-line monitoring:** This scenario targets doctors that will use fog-enabled healthcare products to monitor their patients either at their office or at a patients home during a visit. The patients carry the wearable device at home and then, after a period of time, return the device to their physician to acquire the traces and conduct the diagnosis.

3. **Physician on-line monitoring:** This particular use case is an extension of the previous one, where the patients use the device over an extended period of time and the physician can remotely monitor the acquired vital traces via the available cloud services.

4. **Patient monitoring within Healthcare Infrastructures:** Being the most advanced scenario, this can take place inside an ambulance, hospital or adult day-care center whereby the wearable devices, operated by a personal health assistant instantly acquire the traces of the patient and enable real-time monitoring of the data which are stored to the cloud services.

An example of such application is the **HEART** platform, that combines wearable embedded devices, mobile edge devices, and cloud services to provide on-the-spot, reliable, accurate, and instant monitoring of the heart.

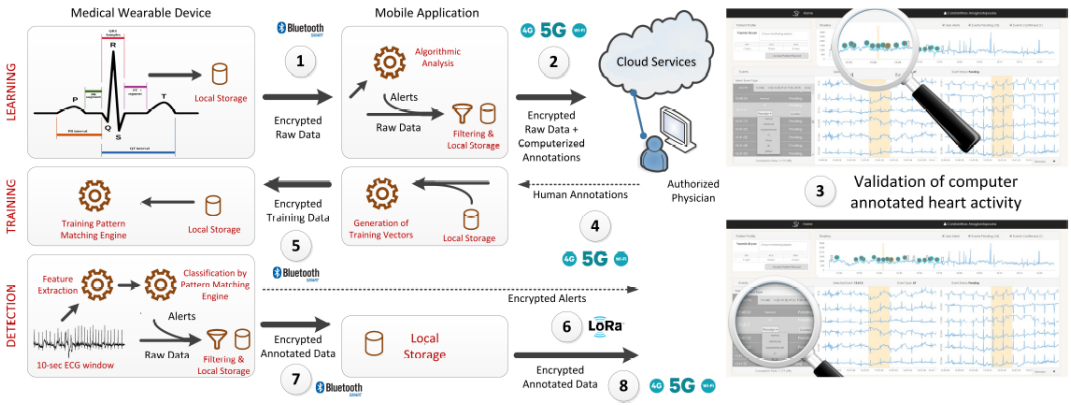

Figure 3.1. Information exchange during the three phases of Learning, Training and Detection

Initially, the wearable ECG goes through a *learning phase* in order to collect an adequate number of ECG recordings based on which we will train the pattern matching engine to match the needs of the particular patient. This is a necessary first step as the evaluation of and ECG depends on anthropometric data (body height and body weight) on age and sex of a patient. During this phase, the wearable device is continuously storing the ECG recordings and periodically forwards them to the nearby edge device. This latter analyzes the received signal and forward it to the cloud services along with computerized annotations. The authorized physician may view reports, search traces and examine ECG alerts aggregated on the patient's health records remotely after they are synced with the cloud platform. The physician goes through the annotated recordings and validates or rejects the computerized

interpretations depending on his expert assessment.
When an adequate number of normal and abnormal sessions have been identified by the authorized physician, the system is ready to enter the *training phase*. The human-curated annotations are forwarded to the edge device where the corresponding sessions are extracted from the local storage, are analyzed to extract a carefully selected set of features. The features of each session along with the annotations constitute the training vectors for the pattern matching engine.
When the training completes, the wearable device is ready to enter the *detection phase*. During the detection phase the signals collected from the ECG leads are analyzed and the features are extracted using the local processor. The resulting vector is passed to the pattern matching engine for classification. In case an abnormal event is detected, the wearable device is in a position to immediately notify the authorized physician via a short message exchange including only the alert type. As soon as the patient visits the physician, the complete ECG recordings are relayed to the nearby edge device. The ECG recordings are finally uploaded on the cloud platform where they become available to the authorized physician for examination and assessment.
The above described cycle of learning, training and detecting is repeated periodically to re-evaluate the operation of the pattern matching of the wearable device and fine-tune its performance. A wearable device that is used for diagnosing and monitoring heart diseases needs to be capable of collecting high-quality ECG traces. During the learning phase, the wearable device is continuously storing the ECG traces on the internal memory. During this offline monitoring period, the device is expected to store a recorded session of 24 hours. For a 12-channel recording produced by sampling 8 leads at 500Hz and a resolution of 16 bit, 24 hours would require about 3.2Gbit memory space. Dropping the sampling rate to 320Hz would reduce the requirements to 2.6Gbit memory capacity.

Table 3.1. ECG trace storage requirements

ECG Trace parameters	Total Size
12 channels, 500 Hz sampling rate	724.3KB
12 channels, 1kHz sampling rate	1.405MB
6 channels, 500 Hz sampling rate	365.414KB
6 channels, 500 kHz sampling rate	722.8KB
2 channels, 360 Hz sampling rate	67.4 KB

During the detection phase, the limiting factors of the operation of the wearable

devices are the standby time achieved. The standby time is directly correlated with:

1. **Battery Performance**
2. **Memory Limitations**

In this way, the independence of the patients is significantly increased. At the same time, continuous communication between patients and their caregivers/physicians is enabled in emergency situations or in cases when the patient requires their full support.
In this context, we implemented a *real-time algorithm* that is a well known adaptive thresholds method developed by *Pan and Tompkins*[12]. We evaluated its performance with respect to the state of the art and, in addition, we measured its computation time on a personal computer and on IoT devices such as a *Raspberry Pi3* and two different *Android* mobile phones.
This algorithm relies on a single ECG lead, that means less battery consumption and memory usage, achieving good results in terms of beat detection accuracy. In most cases, large amounts of data transmitted over the network infrastructure and processed at the cloud level are simply dropped, leading to a significant waste not only of the battery resources of the wearable device but also of network and cloud resources. Hence, it is evident that minimal possible latency, network bandwidth preservation, and efficient data storage resource utilization are elements of paramount importance for any IoT-related application.

3.1 State of the art

	Sensitivity/Recall
Wang, Deepu and Lian [3]	99.82
Zhang [4]	99.83
Sarlija, Jurisic and Popovic [7]	99.81
Van G.V. and Podmasteryev K.V. [29]	98.32
Pan and Tompkins [12]	98.40
Saini, Singh and Khosla [30]	99.8

3.1.1 Wang, Deepu and Lian Algorithm

In the paper [3] a novel Dual-Slope QRS detection algorithm with low computational complexity is presented. The Dual-Slope algorithm calculates the slopes on both sides of a peak in the ECG signal. Moreover, based on these slopes, three criterions are developed for simultaneously checking *steepness of the signal*, *shape of the signal* and *height of the signal* in order to locate each QRS complex.

1. **Steepness of the signal:** The width of QRS complex from the peak to baseline is usually in the range of 0.03-0.05s. Hence, when a sample is processed, only the samples located between 0.03-0.05s away from the current sample are highlighted. Then the slopes of the straight lines connecting the highlighted samples to the current sample are calculated with signs. After that, the maximum and minimum slope on each side are taken and stored. By taking the difference of the two steeper slopes on each side, we can get a variable measuring the steepness of the current processed section. And the first criterion is that this value measuring steepness should be larger than an adaptive threshold.

2. **Shape of the signal:** R peaks usually have steep slopes on both sides. If the *max slope difference* in Criterion 1 is the difference between a flat slope on one side and a very deep slope on the other side, the difference value can be quite high as well. But in this case it should not be considered as a peak. To eliminate this false condition, Criterion 2 is introduced to ensure that the slopes are steep on both sides.

3. **Height of the signal:** Sometimes T wave or P wave or noise sections can produce large slopes as well. However, the heights of these slopes are usually much smaller than those of QRS complex. Hence, by comparing the height of current slope with the average slope height of the previous 8 detected peaks,

wrong detections can be avoided by only accepting the current slope larger than the average.

If a signal section can satisfy all three criterions, a peak should exist in the current section. Then local extremes are searched to locate the peak position, followed by adjustment which aims to avoid multiple detections within the same QRS complex. The proposed algorithm has been implemented in hardware for testing. Based on the implementation, it was found that the total hardware required is very low and therefore is suitable for low power operation in ECG sensors. The algorithm was evaluated against MIT-BIH database and achieved a sensitivity of 99.82%. However, we decided to discard this approach since there was no source-code available and the implementation seemed to be hard.

3.1.2 Zhang Algorithm

This approach is presented in the paper [4]. It is a novel electrocardiograph QRS detection algorithm for wearable ECG devices that utilizes the multistage multiscale mathematical morphology filtering to suppress the impulsive noise and uses the multi-frame differential modulus accumulation to remove the baseline drift and enhance the signal. **Mathematical morphology** is a powerful methodology for the quantitative analysis of geometrical structures. It consists of a broad collection of theoretical concepts, nonlinear signal operators, and algorithms aiming to extract information related to the shape and size from images or other geometrical objects [**?**]. The ECG signal processed by the single-scale operators is similar to an image processed by the gray-scale morphology. This leads to an effective method for detecting the components of interest from the contaminated signal without any prior knowledge about the frequency spectrum which is in sharp contrast to the frequency-based filtering techniques. The elementary single-scale mathematical morphology operators are:

- Dilation
- Erosion
- Opening
- Closing
- Top-hat
- Bottom-hat

QRS complexes are composed of a group of consecutive positive and negative peaks. For what concerns this algorithm, the top-hat operator produces an output consisting of the signal peaks. The bottom-hat operator extracts the valleys (negative peaks). The weighted sum of the top-hat and bottom-hat operations forms a **peak-valley extractor**. Moreover, by using a short structure element in the opening and closing operations, the deterioration of the ECG complexes is avoided whereas the noise is effectively suppressed.

The hardware cost of this kind of filter is much lower than that of **standard filters** (FIR) or wavelets since it does not need the use of the multipliers, that leads to low power consumption. After the filtering, the output ECG sequence is differentiated in order to remove motion artifacts and baseline drifts. Then, the absolute value of the differential output is combined by multiple-frame accumulation, which is very similar to energy transformation [**?**]. Finally, the detection of a QRS complex is accomplished by comparing the feature against a threshold. This threshold is used as the decision function in connection with the proposed transformation for QRS detection. Again, the MIT-BIH Arrhythmia database is used to evaluate the algorithm achieving a detection rate of 99.64%, a sensitivity of 99,83%. We discarded this approach since the implementation seemed to be harder than Pan and Tompkins algorithm and there was no available source-code.

3.1.3 In, Feng, Mang I, Mak Peng Un Algorithm

The approach introduced in this paper [31] is relatively simple but accurate algorithm for QRS detection using a feedforward back propagation artificial neural network for the purposes of improving the diversity of the QRS detection algorithm and fits the trend of the development of QRS detection for battery-driven devices.
Noises from different origin always mix with ECG signal and cause baseline drifts, artifacts and small-scale oscillation. Preprocessing is necessary for the ease of neural network to recognize the QRS complex. The ECG signal is firstly passed through the baseline drifts elimination process and then to a lowpass filter. Baseline drifts elimination is done using two mediane filters, one for removing QRS complexes and P waves while the second for removing the T waves. By subtracting the filtered signal from the original signal, the baseline drifts and artifacts are removed. The lowpass filter can effectively filter the noise which couples from the power supply (60Hz in America), assume that the sampling rate of ECG signal is 360Hz. This assumption bases on the sampling frequency of the recordings of MIT-BIH arrhythmia database, which is 360 Hz.
The input data of the artificial neural network can be the samples of a whole beat, or some features of the beat. In order to reduce the size of the neural network, features of each sample are firstly extracted. This is accomplished by a function called Features Extractor whose inputs are the ECG signal and the number of samples n. The output of Features Extractor is a matrix of three rows of values, which are shown below:

1. The average amplitude of the samples from n - *16* to n + *16*
2. The average of derivatives of samples before n, which are $n-1$, $n-2$, $n-5$, $n-10$, $n-20$, $n-50$, $n-100$
3. The average of derivatives of samples after n, which are $n+1+$, $n+2$, $n+5$, $n+10$, $n+20$, $n+50$, $n+100$

The output of the ANN is just a number which ranges between -1 and 1. By using a Sign function, the positive output values of ANN means the corresponding samples are determined to be R-peaks and the negative output values means the corresponding samples are determined not to be R-peaks.

This approach, tested on the recordings of MIT-BIH arrhythmia database, leads to an accuracy score of 99.5%, but it is not described in which way is the dataset partitioned between training and test set.
Furthermore, the accuracy measure is not relevant and reliable in this context, because of the *accuracy paradox*. In Machine Learning, accuracy is the proportion of correctness in a classification system. The accuracy paradox is the paradoxical finding that accuracy is not a good metric for predictive models when classifying in predictive analytics. This is because a simple model may have a high level of accuracy but it could be too crude to be useful. For example, if the incidence of category A is dominant, being found in 99% of cases, then predicting that every case is category A will have an accuracy of 99%. Hence, precision and recall are better measures for such contexts. Precision and recall measures are more reliable in classification problems in which one or more classes are dominant with respect to others.

3.1.4 Van and Podmasteryev Algorithm

The algorithm for the detection of QRS complexes described in the paper [29] relies on the usage of Support Vector Machine (SVM). The proposed algorithm is then evaluated on the standard well known MIT-BIH Arrhythmia database.
Here, a preliminary processing is applied on the received raw digital ECG signal of a record. Two filters are used, a lowpass filter with a cut-off frequency of 13Hz and a highpass filter with a cut-off frequency of 9Hz, as well as the function of the moving average with a 5 measurements window sizes. Moreover, the filtered signal is squared. Informative feature as rise speed of a signal is chosen, because QRS complex possesses the greatest climb rate. This informative feature is implemented as follows: an array of the values of the slope of the tangent to each point of the filtered and squared ECG signal. After that SVM classification function is applied to the received selection.
Informative feature as correlation forms of QRS-complexes are chosen, because QRS-complex possesses a specific form. This informative feature is implemented as follows: Firstly, test pulse is created based on 1000 QRS-complexes with the R-peak in the middle lasting 51 counting, which occurs after their averaging. Secondly, an array of correlation coefficients forms of QRS-complexes in a moving window is created. After that SVM classification function is applied to the received selection. For the training phase, signal number 100, 104, 200, 205 and 214 are used. The training set consists of 30k values for each of the signs. The function of classification was calculated for each informative feature separately. The main condition for testing algorithm was the use of records which do not participate in training. This was the reason that, if testing is done with the pattern used in learning or training, the accuracy will be artificially high. Signals from MIT-BIH database with 30 min of duration are then used for testing. After testing, a train of 1's is obtained at the output of SVM classifier. Then this train of 1's is picked and by using their duration, average pulse duration of 1's is evaluated. Those trains of 1's, whose duration turns out to be more than the average pulse duration are detected as QRS-complex and the others are discarded.
The QRS detector obtained a sensitivity of 98.32% and a specificity of 95.46%.

3.1.5 Sarlija, Jurisic and Popovic Algorithm

In the paper [7] it is presented a QRS detection algorithm based on pattern recognition as well as a new approach to ECG baseline wander removal and signal normalization.
Each point of the zero-centered and normalized ECG signal is a QRS candidate, while a 1-D CNN classifier serves as a decision rule. Positive outputs from the CNN are clustered to form final QRS detections. The data is obtained from the 44 non-pacemaker recordings of the MIT-BIH Arrhythmia database. The classifier was trained on 22 recordings and the remaining ones were used for performance evaluation.
Traditionally, the preprocessing and filtering of ECG signals based on domain knowledge is used to reduce various forms of noise, remove artefacts, or to limit the signal to a specifically chosen bandwidth. Such approach can give good results, but inherently leads to information loss. In this paper, the preprocessing step is conducted solely to ensure the data is zero-centered and normalized for the classifier training and prediction step. The idea is to have a well extracted ECG morphology, with as little information loss as possible.
The QRS detection strategy is to determine whether a candidate point is a beat or not, based on morphological properties of the ECG signal around the observed point. Every point of the signal was described by a sample of 145 neighbouring points, resulting in a total of 14.296.832 data samples. Each data sample is labelled positive if the candidate point is inside a ±40ms distance of an original positive beat annotation.
The proposed CNN architecture besides a 1-D input layer, consists of two convolutional layers with a max-pooling layer between them, two fully-connected layers and a softmax classification layer. All convolutional and fully-connected layers have a dropout probability of 0.5 to reduce overfitting on training data and make the trained model less sensitive to partial deformations of ECG morphology. Stochastic gradient descent with 0.9 momentum and an initial learning rate of 0.005 was used to train the network. Mini-batch size was 128 samples, and the training was limited to 3 epochs. Input layer also included a zero-centring step, subtracting the training set mean from every sample.
After the classification step, a hierarchical group-average agglomerative clustering upon all CNN decisions of a single recording was performed, with clustering criterion being the temporal euclidean distance with a 80 ms cut-off. Final QRS detection is the mean of all CNN detections within the same cluster. Clusters with less than 5 elements were elected to be too small and were therefore ignored.
To determine whether a detection is a true positive (TP) a ±75ms tolerance window is used. This method achieved a sensitivity of 99.81% and a positive predictive value on unseen data of 99.93%, which is comparable with most of the state-of-the-art solutions.

3.1.6 Saini, Singh and Khosla Algorithm

This work is primarily motivated by the desire to design an algorithm for precise and accurate delineation of QRS-complexes which serves as a reference for the

performance of automated ECG analysis. A raw digital ECG signal of a record is acquired and in order to attenuate noise, it is bandpass filtered. The bandpass filter reduces the influence of muscle noise, 50 Hz interference, baseline wander, and T-wave interference. QRS-complex detection is achieved using gradient as feature. The gradient is a vector, has both direction and units, that points in the direction of the greatest rate of increase of the scalar field, and whose magnitude is the greatest rate of change. In mathematics, gradient is widely used in measuring the degree of inclination, steepness or the rate of ascent or descent. A higher gradient value indicates a steeper incline. Thus it is clear that if the gradient of any signal under test is calculated, then any part of the signal which is having a high slope will have a higher value of gradient. Differentiation allows to find the rate of change. Here in case of ECG signal, it allows to find the rate of change of amplitude of QRS-complex with respect to time samples. Thus, the QRS complex as the most prominent wave component of ECG wave, having high slope and amplitude as compared to the rest of the wave components results in higher value of gradient than non-QRS regions. The gradient at each point in the ECG signal, will show the direction the signal rises most quickly and the magnitude of the gradient will determine how fast the signal rises in that direction. It is not known beforehand which value of K and the type of distance metric are the best for this problem of component wave detection. In the present study fivefold cross-validation approach has been used to select the best K value and type of distance metric. After obtaining the optimal value of K and type of distance metric, the KNN classifier is now trained. The record number 100 of MIT-BIH database was used for training the classifier. The training phase for KNN consists of storing all known instances and their class labels. Here, in this phase, a $[m \cdot n]$ training matrix is formed, consisting of m training instances of n features. The number of training instances (m) is equal to the number of samples of selected portions of ECGs, that is 650.000 for MIT-BIH signals. The value of n, which is the normalized gradient value of each lead of the ECG at a training instance, is equal to 2 since MIT-BIH has signals with two leads. If the training instance belongs to a QRS region, the training label vector is set to 1 and if it belongs to non-QRS region it is set to -1. Whole file of 30 minutes duration is used for testing. After testing, a train of 1's is obtained at the output of KNN classifier. Then this train of 1's is picked and by using their duration, average pulse duration of 1's is evaluated. Those trains of 1's, whose duration turns out to be more than the average pulse duration are detected as QRS complex and the other are discarded.
In order to obtain the final results, the algorithm has been applied to MIT-BIH Arrhythmia database for QRS detection, achieving a sensitivity score of 99,81%.
An alternative to this solution consists in considering a feature vector corresponding to a time segment, i.e. a window. The algorithm determines for each window whether it is a QRS wave or not. The signal is therefore segmented in equally sized and contiguous windows. Consequently, each segment in the training set is labeled according to the database annotations ih the following way:
$\forall$ *segment s in X_train*:

$$label(s) = \begin{cases} 1 & if\ s\ contains\ a\ QRS\ annotation \\ -1 & otherwise \end{cases}$$

The QRS detection output consists on the classifier predictions for each unseen region in the test set.
The segments to which corresponds a positive prediction(+1) are the ones which presumably contains a QRS wave.
The R peak location is then detected from such regions by applying the following formula:

$$rpeak\_location = argmax(abs(region))$$

Since not all the annotations of the R peak locations in the MIT-BIH database are placed precisely on the maximum of the QRS wave, a peak detection is considered correct if it resides inside a range of 0.1s around the real peak annotation. Applying this technique, the achieved sensitivity score is equal to 93.8%. From now on, we will refer to this approach with the name *QRS KNN*.

3.2 Signal Processing

We consider a record as a structure composed by a number (n) of channels, therefore the vector is n-dimensional.
The elements of the channels, representing the amplitude of the signal at any given time, are named *samples*.
A channel is the signal recorded from a specific lead configuration. (see Subsection 2.2)

3.2.1 Positive Normalization Technique

This preprocessing technique has been adopted in the *First Order Difference* algorithm (see Section 3.3.1).
Since this is a standard algorithm, the preprocessing phase has not the objective of improving the performance of the algorithm but just to adapt the input data.
The implementation used to generate the results, named *PeakUtils*[13], requires a positive normalized signal as input.
This means that every amplitude of the signal must be in the positive and in the range [0,1].
In order to achieve this, a max normalization is performed: each sample of the signal is divided by the value of the maximum amplitude.
After that transformation, the maximum of the signal will have a resulting amplitude of 1, and the values corresponding to the other samples will represent the amplitude in percentage with respect to the maximum.
The whole process is formally expressed by:

$$sample = \frac{abs(sample)}{\max(abs(signal))}$$

3.2.2 Filtering and Squaring Techniques

QRS detection is a difficult task, not only because of the physiological variability of the QRS complexes inter-patients and intra-patients but also because of the various types of noise that can be present in the ECG signal. [12]
Noise sources include muscle noise, artifacts due to electrode motion, power-line interference, baseline wander, and T waves with high-frequency characteristics similar to QRS complexes.
In our approach, digital filters are used to reduce the influence of these noise sources.
We initially passed all the signals through a **bandpass filter**. Such filter reduces the influence of muscle noise, 60 Hz interference, baseline wander, and T-wave interference. The desirable passband to maximize the QRS energy is approximately 5-15 Hz.[12]
It is implemented with a cascade of low-pass and high-pass filters to achieve a 3dB passband from about 5-12 Hz, reasonably close to the desirable passband.
The transfer function of the second-order low-pass filter is :

$$H(z) = \frac{(1-z^{-6})^2}{(1-z^{-1})^2}$$

The amplitude response is:

$$|H(wT)| = \frac{sin^2(3\omega T)}{sin^2(\frac{\omega T}{2})}$$

where T is the sampling period. The difference equation of the filter is:

$$y(nT) = 2y(nT - T) - y(nT - 2T) + x(nT) - 2x(nT - 6T) + x(nT - 12T)$$

where the cutoff frequency is about 11Hz and the gain is 36. The filter processing delay is six samples. The design of the high-pass filter is based on subtracting the output of a first-order low-pass filter from an all-pass filter (samples in the original signal). The transfer function for such a high-pass filter is:

$$H(z) = \frac{-1+32z^{-16}+z^{-32}}{1+z^{-1}}$$

The amplitude response is:

$$|H(wT)| = \frac{[256+sin^2(16\omega T)]^{\frac{1}{2}}}{cos(\frac{\omega T}{2})}$$

The difference equation is:

$$y(nT) = 32x(nT - 16T) - [y(nT - T) + x(nT) - x(nT - 32T)$$

The low cutoff frequency of this filter is about 5Hz, the gain is 32 and the delay is 16 samples. After filtering, the signal is differentiated to provide the QRS-complex slope information. We used a five-point derivative with the transfer function:

$$H(z) = (\frac{1}{8T})(-z^{-2} - 2z^{-1} + 2z + z^2)$$

The amplitude response is:

$$|H(wT)| = (\frac{1}{4T})[sin(2\omega T) + 2sin(\omega T)]$$

The difference equation is:

$$y(nT) = (\frac{1}{8T})[-x(nT - 2T) - 2x(nT - T) + 2x(nT + T) + x(nT + 2T)]$$

The frequency response of this derivative is nearly linear between dc and 30Hz. Its delay is two samples.
After differentiation, the signal is squared point by point. The equation of this operation is:

$$y(nT) = [x(nT)]^2$$

In this way, all data points turn to be positive and we obtain a nonlinear amplification of the output of the derivative, emphasizing the higher frequencies (i.e., predominantly the ECG frequencies and the QRS complex in particular). The result of the preprocessing stage is shown step-by-step in the following pictures having samples on X-axis and signal amplitude on Y-axis:

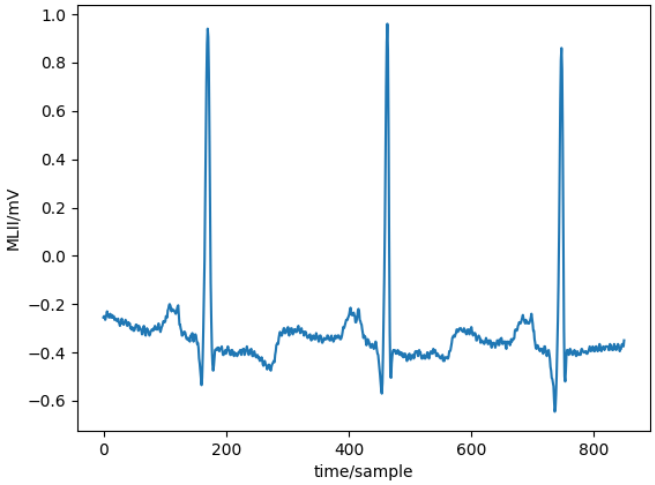

Figure 3.2. Raw Signal

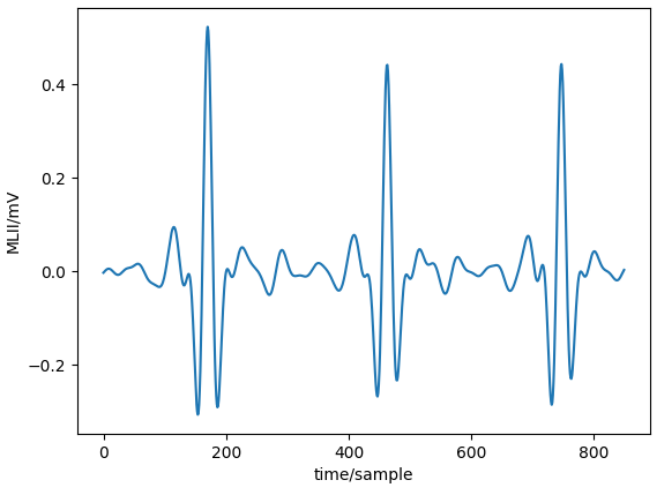

Figure 3.3. Filtered Signal

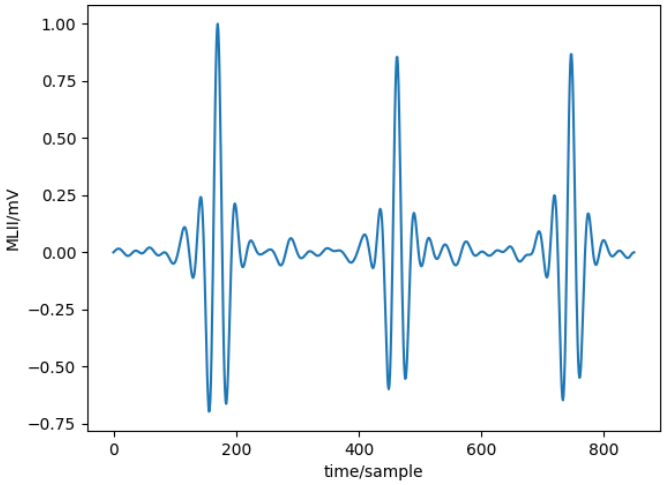

Figure 3.4. Derived Signal

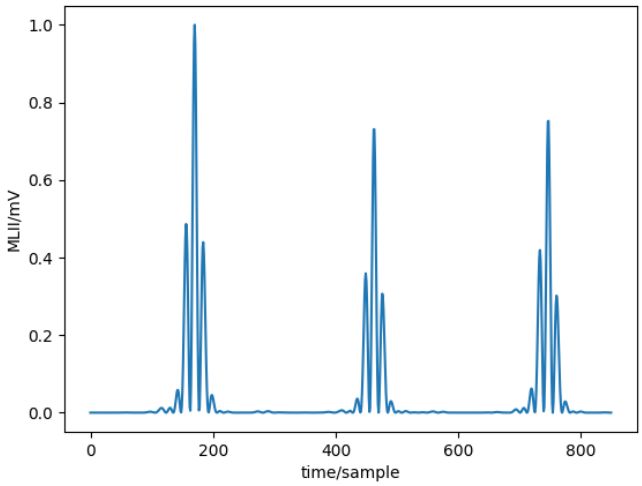

Figure 3.5. Squared Signal

3.3 R Peak Detection Algorithms

3.3.1 First-Order Difference Algorithm

In this context, the first order difference in the signal, i.e. the first derivative [13], is defined as follows :

$$y'(n+1) = y(n+1) - y(n)$$

The locations of the local maxima, i.e. the candidate **R Peak indexes**, correspond to the ones that satisfy the following conditions:

- The first order difference is zero, $y'(n) = 0$
- The previous and the subsequent value of the point, are of discordant sign: $y'(n-1) - y'(n+1) < 0$ *or* $y'(n+1) - y'(n-1) < 0$

These conditions lead to the detection of points in which a curvature of the original function occurs, the presumed R peak locations.
Such computation is refined with the tuning of the following parameters:

- **Threshold :** Only the peaks with amplitude higher than the threshold will be detected.
- **Minimum Distance:** Minimum distance between each detected peak.

From a medical point of view, the physiological minimum distance between two heartbeats is 0.2s that in our case corresponds to 72 samples [12].

3.3.2 Pan and Tompkins Algorithm

This is a real-time algorithm for detection of the QRS complexes on ECG signals.[12] QRS detectors typically include one two different types of processing steps: preprocessing and decision [32]. Preprocessing includes linear digital filtering and non-linear transformation.

- **Linear Digital Filtering:** In signal processing, a linear digital filter is a system that performs mathematical operations on a sampled signal, subject to the constraint of linearity, in order to reduce or enhance certain aspects of that signal. For what concern this algorithm, the linear process includes a bandpass filter, a derivative filter and a moving window integrator.
- **Non-Linear Transformation:** A nonlinear transformation changes the correlation between variables. In our case, the nonlinear transformation corresponds to the signal amplitude squaring (see Section 3.2.2).

- **Decision Rule Algorithms:** In decision theory, a decision rule is a function which maps an observation to an appropriate consequence. In this algorithm, adaptive thresholds and T-wave discrimination techniques turn the algorithm into a decision rule based algorithm.

Pan and Tompkins's method has been found to have the higher accuracy for different beat shapes than other real-time approaches developed before 1990.[33].
The algorithm is divided into three phases:

1. **Learning phase 1:** It requires about 2s to initialize detection thresholds based upon the signal and noise peaks detected during the learning process
2. **Learning phase 2:** It requires two heartbeats to initialize RR-interval average and RR-interval limit values, where RR is the distance between two consecutive R waves.
3. **QRS Detection:** This phase does the recognition process and produces a pulse for each QRS complex. Once a peak is located, it must be classified as a signal peak or as a noise peak. To be a signal peak, the peak must exceed the higher threshold as the signal is first analyzed or it must exceed the lower threshold if the search-back approach is required to find a QRS complex.

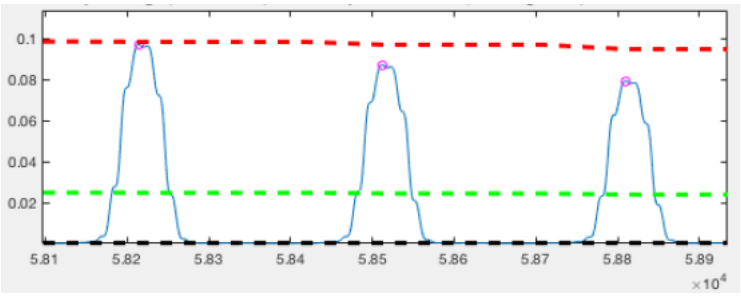

Figure 3.6. Higher (red) and lower (green) thresholds for the original signal

The algorithm applies the preprocessing techniques described in section 3.2.2 and, in addition, apply a moving window integration. The purpose of moving-window integration is to obtain waveform feature information in addition to the slope of the R wave. It is calculated from:

$$y(nT) = (\tfrac{1}{N})[x(nT-(N-1)T) + x(nT-(N-2)T) + \cdots + x(nT)]$$

where N is the number of samples in the width of the integration window and T is the sampling period. The number of samples N in the moving window is important. Generally, the width of the window should be approximately the same as the widest possible QRS complex. If the window is too wide, the integration waveform will merge the QRS complex and T wave together. If it is too small, some QRS complex will produce several peaks in the integration waveform.
The QRS complex corresponds to the rising edge of the integration waveform. The time duration of the rising edge is equal to the width of the QRS complex. A fiducial

mark for the temporal location of the QRS complex can be determined from this rising edge according to the desired waveform feature to be marked such as the maximal slope or the peak of the R wave.
During the execution of the algorithm, the thresholds and other parameters of the algorithm are adjusted periodically to adapt to changing characteristics of the signal. There are two sets of thresholds to detect QRS complexes. One set thresholds the filtered ECG while the second thresholds the signal produced by moving window integration.
The higher of the two thresholds in each of the two sets is used for the first analysis of the signal. The lower threshold is used if no QRS is detected in a certain time interval so that a search-back technique is necessary to look back in time for the QRS complex. The set of thresholds initially applied to the integration waveform is computed from:

$$SPKI = 0.125 \cdot PEAKI + 0.875 \cdot SPKI \text{ if PEAKI is the signal peak}$$
$$NPKI = 0.125 \cdot PEAKI + 0.875 \cdot NPKI \text{ if PEAKI is the noise peak}$$
$$THRESHOLDI1 = NPKI + 0.25 \cdot (SPKI - NPKI)$$
$$THRESHOLDI2 = 0.5 \cdot THRESHOLDI1$$

where all the variables refer to the integration waveform:

- **PEAKI:** is the overall peak
- **SPKI:** is the running estimate of the signal peak
- **NPKI:** is the running estimate of the noise peak
- **THRESHOLDI1:** is the first threshold applied
- **THRESHOLDI2:ÂăÂă**is the second threshold applied

A peak is a local maximum determined by observing when the signal changes direction within a predefined time interval. The signal peak SPKI is a peak that the algorithm has already established to be a QRS complex. The noise peak NPKI is any peak that is not related to the QRS (e.g. a T wave).
When a new peak is detected, it must first be classified as a noise peak or a signal peak. To be a signal peak, the peak must exceed THRESHOLDI1 as the signal is first analyzed or THRESHOLDI2 if searchback is required to find the QRS.
Unfortunately, the dual-threshold technique is only useful if the heart rate is regular. For the case of irregular heart rates, the first threshold of each set is reduced by half so as to increase the detection sensitivity and to avoid missing beats. To be identified as a QRS complex, a peak must be recognized as such a complex in both the integration and bandpass-filtered waveforms.
Moreover, two RR-interval averages are maintained.

- **RR AVERAGE 1:ÂăÂă**average of the eight most recent beats
- **RR AVERAGE 2:** average of the eight most recent beats having RR intervals that fall within certain limits

The reason for maintaining these two separate averages is to be able to adapt to quickly changing or irregular heart rates. If a QRS complex is not found during the interval specified by the RR MISSED LIMIT = 166% RR AVERAGE 2, the maximal peak reserved between the two established thresholds is considered to be a QRS candidate.
If each of the eight most recent sequential RR intervals that are calculated from RR AVERAGE1 is between the RR LOW LIMIT = 92%RR AVERAGE 2 and the RR HIGH LIMIT = 116% RR AVERAGE 2, we interpret the heart rate to be regular for these eight heart beats and RR AVERAGE 2 = RR AVERAGE 1.
Once a valid QRS complex is recognized, there is a 200ms **refractory period** [12] before the next one can be detected. This refractory period eliminates the possibility of a false detection such as multiple triggering on the same QRS complex during the time interval.
When a QRS detection occurs after the end of the refractory period but within 360 ms of the previous complex, it is important to understand if the candidate QRS is a valid QRS complex or a T wave. In this case, if the maximal slope that occurs during this waveform is less than half that of the QRS waveform that preceded it, it is identified to be a T wave; otherwise, it is called a QRS complex.

3.4 Evaluation

Since not all the annotations of the R peak locations in the database are placed precisely on the maximum of the QRS wave but guaranteed to be inside it, we could not use them as we find them in the database for the evaluation purpose.
For this, a peak detection is considered **correct** if it resides inside a range of 0.1s around the real peak annotation.
Such amount of sample is chosen to be comparable to the average QRS width.([34], Chapter 2, Section 41)
According to this definition of correctness, we evaluate the performance of the proposed algorithms with the following measures:

$$Precision = \frac{|correctly\ detected|}{|detected|}$$
$$Recall = \frac{|correctly\ detected|}{|real\ peaks|}$$

3.4.1 Database

The database taken into account for the evaluation of this study is the *MIT-BIH Arrhythmia Database*[35]. This database was the first generally available set of standard test material for evaluation of arrhythmia detectors, and it has been used for that purpose as well as for basic research into cardiac dynamics. MIT-BIH arrhythmia database is a collection of annotated ECG recordings obtained by the Arrhythmia Laboratory of Boston's Beth Israel hospital. From such collection, 48 half-hour excerpts of two-channel, 24 hours, ECG recordings obtained from 47 subjects (record 201 and 202 are from the same subject) have been selected.
The signals are divided into *100 series*, 23 signals chosen at random from a collection of over 4000 Holter tapes, and *200 series*, 25 signals selected to include examples of uncommon but clinically important arrhythmias that would not be well represented in a small random sample.
The subjects included 25 men aged 32 to 89 years and 22 women aged 23 to 89 years; approximately 60% of the subjects were inpatients. The ECG leads varied among subjects as would be expected in clinical practice, since surgical dressings and variations in anatomy do not permit use of the same electrode placement in all cases. In most records, one channel is a modified limb lead II (MLII), obtained by placing the electrodes on the chest as is standard practice for ambulatory ECG recording, and the other channel is usually V1 (sometimes V2, V4 or V5, depending on the subject).
Five years were needed to complete the MIT-BIH Arrhythmia Database. The digitization rate, that is 360 samples per second per channel) was chosen to accommodate the use of simple digital notch filters to remove 60 Hz interference. Each recording of the MIT-BIH Arrhythmia Database corresponds to a 2D vector of 650K entries. The vector is composed of two channels, therefore it is two dimensional. Moreover, four of the 48 recordings include paced beats, i.e. produced by a pacemaker.

3.4.1.1 Annotations

Once the digital tapes had been prepared, they have been annotated using a simple slope-sensitive QRS detector. Each half-hour tape was used to produce two identical 46m paper chart recordings. Then, these charts for each recording were given to two cardiologists, who worked independently, adding additional beat labels and deleting false detections as necessary, and changing the labels for abnormal beats.
The cardiologists also added rhythm and signal quality labels. At this point the two sets of annotations were compared automatically and another chart recording was printed, showing the cardiologists' annotations in the margin, with all discrepancies highlighted. Each discrepancy was examined and resolved by consensus.
Approximately $110,000$ annotations were created and verified in this way. Notably, six of the 48 records contain a total of 33 beats that remain unclassified because the cardiologist-annotators were unable to reach agreement on the beat types. In the end, every QRS complex was annotated, about $109,900$ in all.
The list of annotations present in the database are described later:

Table 3.2. Beat annotations

Beat Annotations	
Symbol	Meaning
N	Normal Beat
R	Right bundle branch block beat
L	Left bundle branch block beat
A	Atrial premature beat
a	Aberrated atrial premature beat
J	Nodal (junctional) premature beat
S	Supraventricular premature beat
V	Premature ventricular contraction
F	Fusion of ventricular and normal beat
[	Start of ventricular Flutter/Fibrillation
!	Ventricular flutter wave
]	End of ventricular Flutter/Fibrillation
e	Atrial escape beat
j	Nodal (junctonal) escape beat
E	Ventricular escape beat
/	Paced beat
f	Fusion of paced and normal beat
x	Non-conducted P-wave (blocked APB)
Q	Unclassifiable beat
|	Isolated QRS-like artifact

Table 3.3. Rhythm Annotations

Rhythm Annotations	
Symbol	Meaning
(AB	Atrial bigeminy
(AFIB	Atrial fibrillation
(AFL	Atrial flutter
(B	Ventricular Bigeminy
(BII	Second degree AV Block
(IVR	Idioventricular rhythm
(N	Normal sinus rhythm
(NOD	Nodal (AV junctional) rhythm
(P	Paced rhythm
(PREX	Pre-excitation (WPW)
(SBR	Sinus bradycardia
(SVTA	Supraventricular tachyarrhythmia
(T	Ventricular Trigeminy
(VFL	Ventricular Flutter
(VT	Ventricular Tachycardia

3.5 Protocol Fine-Tuning

For what concern Pan and Tompkins method there were no parameters to train the method on since this algorithm just need the ECG signal and the frequency sampling rate as inputs.
However, we report all the combinations of parameters studied and the obtained score, in order to select the best ones for the FOD heartbeat detection algorithm. We tried out different threshold values, precisely in a range from 0.1 to 1 with a step of 0.1.
The result, still measured according to precision and recall (see Section 3.4), is in the picture below:

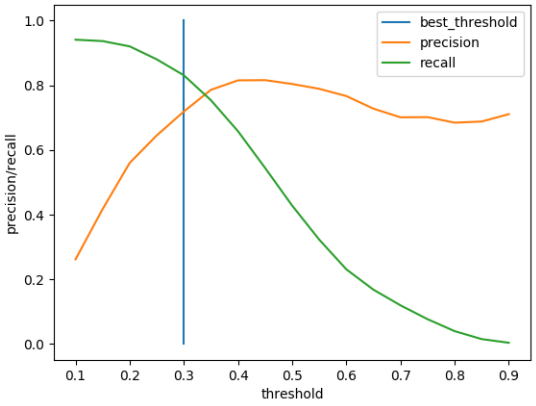

Figure 3.7. Precision and Recall for different normalized threshold values

Hence, the best threshold value is 0.3. This means that every sample with amplitude less than 0.3 mV after the preprocessing stage (see Subsection 3.2.1) cannot be detected as a peak.

3.6 Comparative Evaluation

Once we had the results from all the algorithms, we decided to compare them in order to find out the best R peak detection algorithm. The first objective we wanted to achieve was that of proving that the preprocessing phase is effectively useful for the specific QRS detection task. Hence, we evaluated the same algorithms in terms of precision and recall giving them as input both the raw and filtered signals.
Moreover, we analyzed the performances of the algorithms with respect to the number of leads used in input. This was not possible to apply to the Pan and Tompkins approach since it needs a one-dimensional vector as input.
From now on, we will refer to each combination we tried out with the following schema $xx\_yy\_ww\_zz$ that means:

- **xx:** This is the name of the approach. We will refer to Pan and Tompkins approach with PT, to the First Order Difference algorithm with FOD and to the KNN approaches with KNN.

- **yy:** This label refers to both the approaches used for KNN, mentioned in subsection 3.1.6, where w stands for QRS KNN and s to the standard approach suggested in the paper [**?**]

- **ww:** This label actually describes the elaboration of the input data. This can be RS (raw signal) if no preprocessing techniques are applied or FS (filtered signal) if the signal is elaborate through the preprocessing phase

- **zz:** Here we have three different options, "1" means that only the first channel is considered, "2" means that only the second channel is considered and "B" means that both channels are considered.

Table 2: Approaches Comparison

APPROACH	PRECISION	RECALL
FOD_RS_1	0.817	0.768
FOD_RS_2	0.574	0.676
FOD_FS_1	0.301	0.973
FOD_FS_2	0.319	0.834
KNN_s_RS_1	0.347	0.457
KNN_s_RS_2	0.237	0.313
KNN_s_RS_B	0.304	0.632
KNN_s_FS_1	0.371	0.825
KNN_s_FS_2	0.392	0.686
KNN_s_FS_B	0.322	0.588
KNN_w_RS_1	0.926	0.843
KNN_w_RS_2	0.893	0.744
KNN_w_RS_B	0.93	0.852
KNN_w_FS_1	0.988	0.923
KNN_w_FS_2	0.924	0.807
KNN_w_FS_B	0.988	0.924
PT_FS_1	0.984	0.984
PT_FS_2	0.708	0.715

LEGEND:

FOD = First Order Difference .
KNN = KNN .
PT = Pan and Tompkins
w = Window approach for KNN.
s = Sampled approach for KNN.
RS = Raw Signal.
FS = Filtered Signal.
1 = First Channel selected.
2 = Second Channel selected.
B = Both First and Second channel selected.

The results shown above clearly declare the efficiency of elaborating data with preprocessing techniques, except for the First Order Difference algorithm. It is easy to see that the generic algorithm for analyzing signals peak performs worse than a specific procedure implemented for the specific task of QRS detection.

The machines we executed the algorithm on, for running all the combinations, have the following technical specifications:

1. Computer:
   - **Processor:** Intel(R) Core(TM) i3-3240 CPU @3.40GHz, 4 cores
   - **RAM:** 4 GB
   - **Operative System:** Ubuntu 16.04
   - **Linux Kernel:** 4.4
2. Raspberry:
   - **Processor:** Arm Cortex-A53 CPU @2.1GHz, 4 cores
   - **Ram:** 1 GB
   - **Operative System:** Android 4.4.2
   - **Linux Kernel:** 4.4
3. Android phone:
   - **Processor:** Qualcomm SnapDragon 600 CPU @1.9 GHz, 4 cores
   - **Ram:** 2 GB
   - **Operative System:** Android 4.4.2
   - **Linux Kernel:** 3.4
4. Android phone:
   - **Processor:** Arm Cortex-A53 CPU @2.1 GHz, 4 cores, @1.7 GHz, 4 cores
   - **Ram:** 3 GB
   - **Operative System:** Android 7.0 Emotion UI v5.0 Nougat
   - **Linux Kernel:** 4.1.18

We tried out all the combinations (see Table 2) and plotted the top5 recall scores for those approaches that has a precision score higher than 90%.

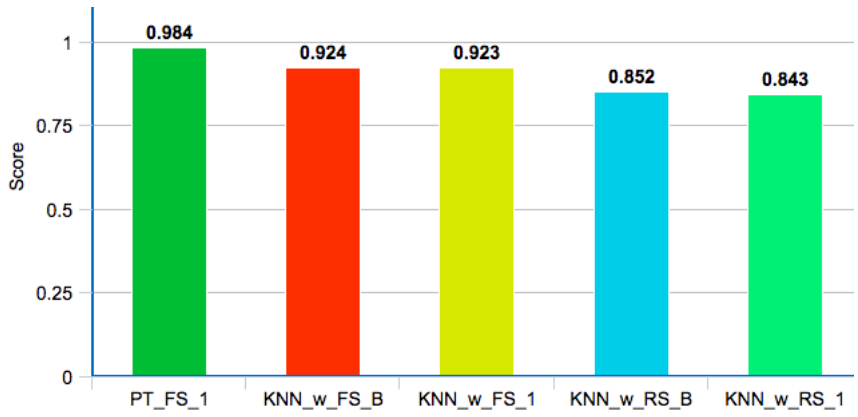

Figure 3.8. Top 5 Algorithms' performances ordered from the best (left) to the worst (right) in terms of recall

As we can see from the chart, the algorithm that achieves the best results is the Pan and Tompkins algorithm. On the other hand, the worst one, as we could have expected since it was not implemented as an R-peak detector but only as a peak detector, is the generic algorithm provided by *PeakUtils*.
Moreover, we measured the computational time of all the algorithms where the elapsed time is computed as the time for processing a single sample out of 650000 entries for all the 48 signals, that is the amount of time needed to declare if a certain sample represents an R peak or not. More precisely, in order to apply this evaluation to other databases, the formula described above is :

$$single\_sample\_computational\_time = \frac{time}{samples}$$

where time is the total time to analyze a whole signal and samples is the total number of samples in the whole signal.
From now on, we will take into account the implementation from scratch of the KNN since it will be useful for working on Android. In the following table, we show the comparison between the machines we worked on, in terms of elapsed time. Note that, of course, the precision and recall scores will be omitted since they are equivalent for both machines because they do not depend on the technical specifications.

Table 3.4. RAM usage and elapsed time measured in millisecond for each combination

	elasped time (ms)				Ratio Cortex/Intel	Ratio	Ratio	Ratio Cortex 8 cores/	RAM usage (MB)
Processor	Intel(R) Core(TM) i3-3240 CPU @3.40GHz, 4 cores	Arm Cortex-A53 CPU @2.1GHz, 4 cores	Qualcomm Snapdragon 600 CPU @1.9 GHz, 4 cores	Arm Cortex-A53 CPU @2.1GHz, 4 cores @1.7GHz, 4 cores		Qualcomm/Intel	Qualcomm/Cortex 4 cores	Cortex 4 cores	
FOD_RS_1	0.00639	0.0611	0.0603	0.0217	9,56	9,43	0,98	0,35	92,372
FOD_RS_2	0.00651	0.0629	0.0605	0.0273	9,66	9,29	0,96	0,43	91,832
FOD_FS_1	0.000180	0.00274	0.0743	0.00332	15,22	412,77	27,11	1,21	92,424
FOD_FS_2	0.000181	0.00204	0.0789	0.00329	11,27	435,91	38,67	1,61	92,025
KNN_s_RS_1	70.350	466.34	672.51	880.00	6,629	9,559	1,442	1,887	127,594
KNN_s_RS_2	64.616	479.79	698.15	892.00	7,425	10,805	1,455	1,859	120,245
KNN_s_RS_B	87.273	1980.1	1705.1	1983.0	22,689	19,538	0,861	1,001	139,637
KNN_s_FS_1	110.45	1154.3	1036.3	1046.0	10,451	9,383	0,898	0,906	138,639
KNN_s_FS_2	105.55	703.54	1026.4	1060.0	6,665	9,724	1,46	1,507	137,461
KNN_s_FS_B	127.52	2556.8	2178.4	2228.0	20,05	17,083	0,852	0,871	181,993
KNN_w_RS_1	0.0029	0.0219	0.0531	0.0504	7,552	18,31	2,425	2,301	109,227
KNN_w_RS_2	0.0032	0.0211	0.0693	0.0499	6,594	21,65	3,28	2,365	109,637
KNN_w_RS_B	0.0044	0.0392	0.8	0.0919	8,909	181,81	20,4	2,344	128,618
KNN_w_FS_1	0.0031	0.0212	0.0662	0.0499	6,839	21,355	3,122	2,354	127,34
KNN_w_FS_2	0.0032	0.0212	0.0519	0.0501	6,625	16,22	2,448	2,363	110,14
KNN_w_FS_B	0.0049	0.0379	0.1	0.0911	7,735	20,4	2,63	2,404	129,03
PT_FS_1	0.0009711	0.004693	0.01211	0.00836	4,83	12,47	2,58	1,78	99,92
PT_FS_2	0.0009576	0.004620	0.011993	0.00827	4,82	12,52	2,59	1,79	102,21

As described in 3.4.1, we know that each signal of the MIT-BIH Arrhythmia Database has a sampling rate of 360 Hz, that means that a single sample is processed every 3ms ($\frac{1}{360}s \cdot 10^3$). If the computational time taken by an algorithm to declare if a unique sample represents an R peak or not is less than this value, then the algorithm is executable in real time.
In addition, we measured the amount of RAM used to process one signal to understand if it was feasible to run each combination on all the machines, according to their technical specifications.

In the following chart are shown the elapsed time on the *Intel(R) Core(TM) i3-3240 CPU @3.40GHz 4 cores* of each of the top5 algorithms in terms of recall.

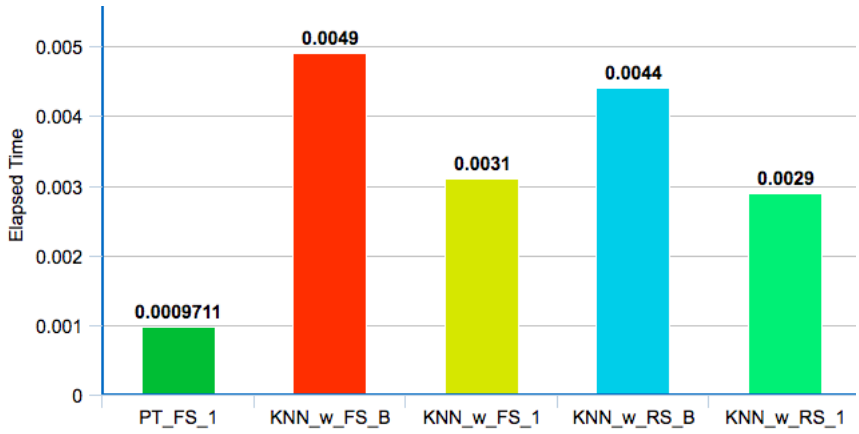

Figure 3.9. Top 5 Algorithms' elapsed time

From this chart it is easy to understand that each of these 5 combinations, that are the fastest ones, can operate in real time.
In the next figure it is described a comparison between the best result obtained for each algorithm in terms of recall.

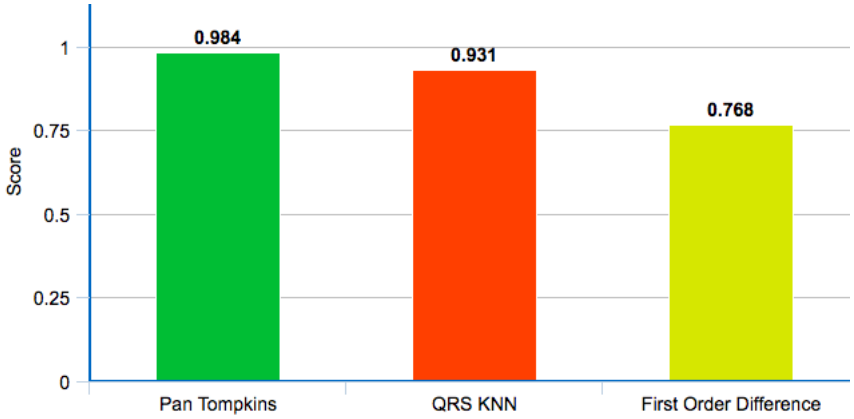

Figure 3.10. Recall score for the best combination of each algorithm

The Pan and Tompkins approach using one channel and filters included in the preprocessing achieves the best performances in terms of recall and, in addition, has also the minimum computation time.

3.7 Critical Issues

In this section we analyze the most common cases in which the algorithm fail in the peak detection and we try to understand the reason why it happened.

3.7.1 Example 1: First Order Difference Algorithm

In the figure below we can see a detected peak from the *First Order Difference* algorithm (Subsection 3.3.1) in the signal '102' of the 'MIT-BIH Arrhythmia Database'.

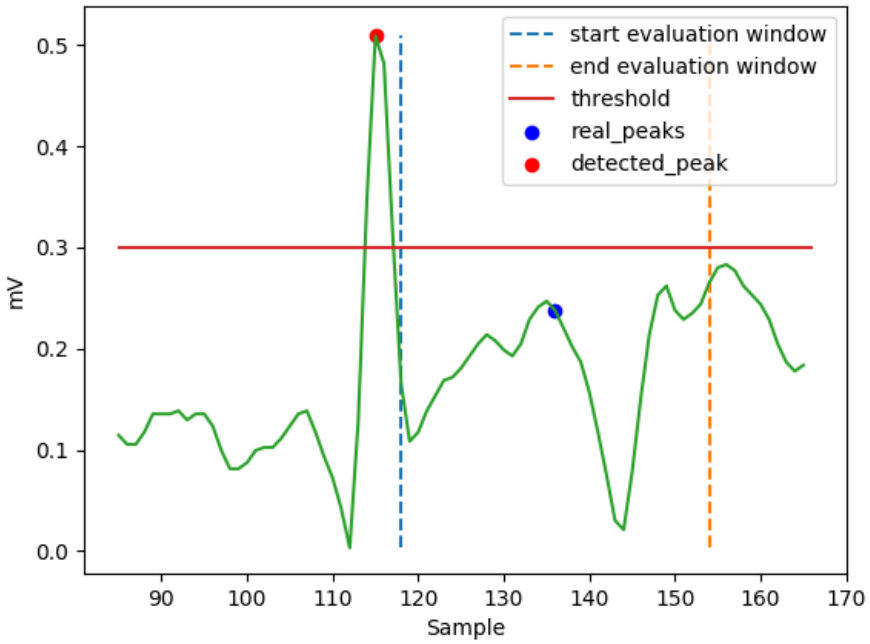

Figure 3.11. Generic Algorithm Wrong R Peak detection

As explained in section 3.4, this detection is not correct because the peak detected does not reside in the evaluation window, which is of 0.1s around the annotation, which corresponds to 36 samples in this context.
Recall that the signal in the plot is the absolute value of the signal normalized;
We deduce that, after this transformation, the amplitude of the real peak is lower than the algorithm threshold (see Section 3.5) and therefore it cannot be detected.

3.7.2 Example 2: Pan and Tompkins algorithm

In the figure below we can see two detected peaks from the Pan and Tompkins algorithm in the signal *101* of the MIT-BIH Arrhythmia Database.

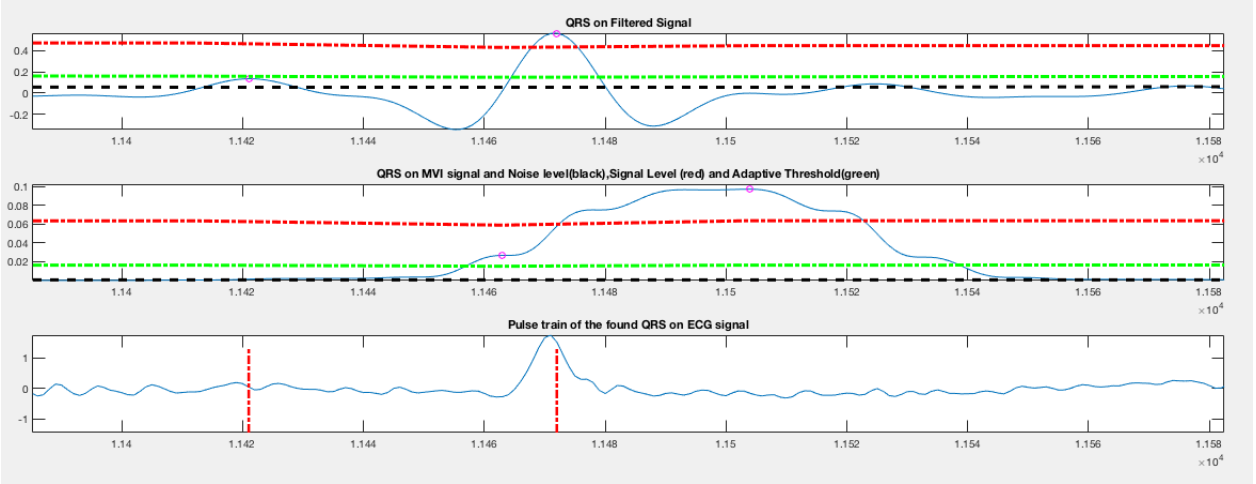

Figure 3.12. Pan and Tompkins Algorithm Wrong R Peak detection

As we can see from the picture, we have two detected peaks, located at 11421 and 11472. In the first chart, representing the QRS detection on filtered signal, the peak located at 11421 is clearly lower than the higher threshold used during the first analysis of the signal. Moreover, we can see that it is also lower than the lower threshold (green dashed line).
However, it is classified as a peak since, when using the moving window integration technique, the signal is slightly enhanced and shifted to the right. This will shift the candidate peak between the two thresholds and it will let the peak be classified as a real signal peak.
We could actually avoid this by re-applying a minimum distance analysis between each detected peak, since, as we know, the minimum samples distance between two different peaks in our case is 72 (0.2 * 360, where 360 is the frequency sampling and 0.2 the refractory period) [12]. In this case, the two detected peaks are separated by 51 samples so this error would be avoided, reducing the number of false positives.
The decision about which of the two peaks, in a range smaller than 72 sample, should be chosen as real signal peak could be solved by taking the candidate peak with higher amplitude.

Chapter 4

Arrhythmia Detection and Classification

Arrhythmia can be defined as either an irregular single heartbeat (arrhythmic beat), or as an irregular group of heartbeats (arrhythmic episode). Arrhythmia can take place in healthy heart and be of minimal consequence, as the case of respiratory sinus arrhythmia which is a natural periodic variation in heart rate corresponding to respiratory activity, but they may also indicate a serious problem that may lead to stroke or sudden cardiac death, e.g. ventricular fibrillation episode. For this reason, automatic arrhythmia detection and classification is critical in clinical cardiology, especially when performed in real time. The electrocardiogram is the record of variation of bio-electric potential with respect to time as the human heart beats. Interpretation of ECG patterns is needed for diagnosing malfunctions of the human heart. Ventricular heart rate is the most common item of information among those which can be extracted from the ECG tracing of the human heart by measuring the time distance between two successive R peaks. It is required for detection of ventricular fibrillation and other life-threatening arrhythmias or abnormal cardiac rhythms [38].

The sooner is the detection of arrhythmias, the greater is the chance of recovery. This is really important because it was observed that life-threatening arrhythmias were usually preceded by less-severe premonitory arrhythmias [37], and by timely detection and proper therapeutic treatment of the latter, the occurrences of the former might be avoided.

Usually, computer-based ECG interpretation performs classification of ECG patterns after extracting necessary wave features from the preprocessed digitized ECG patterns. Some techniques are based on the detection of a single arrhythmia type and its difference from normal sinus rhythm, or the discrimination between several kinds of arrhythmia. Quite all methods address the detection of only a few types of arrhythmias such as atrial tachycardia, ventricular tachycardia, atrial fibrillation and ventricular fibrillation.

Most of the studies are based on the analysis of the ECG signal. In these methods, ECG features are extracted and used for the detection and/or classification of arrhythmias. However, this is not always possible due to the time consuming that could make the approach ineffective for real-time analysis.

The method we implemented is a decision rule algorithm developed by Tsipouras et Al. [14] that classify cardiac rhythms taking as input just the RR intervals of a signal.
This algorithm proposes a knowledge-based method for arrhythmic beat classification and arrhythmic episode detection and classification. A three RR-interval sliding window is used in arrhythmic beat classification algorithm. Classification is performed for four categories of beats:

1. **Normal Beat**
2. **Premature Ventricular Contraction**
3. **Ventricular Fibrillation**
4. **Second Heart Block**

The beat classification output is used as input of a knowledge-based deterministic automaton to achieve arrhythmic episode detection and classification. Six rhythm types are classified:

1. **Ventricular Bigeminy**
2. **Ventricular Trigeminy**
3. **Ventricular Couplet**
4. **Ventricular Tachycardia**
5. **Ventricular Fibrillation**
6. **Second Heart Block**

A rule-based classification algorithm is simple and fast in computation by only measuring the time intervals between each of the R peaks. The method takes as input peaks' locations retrieved with the algorithm introduced in chapter 3. The proposed knowledge-based system consists of three phases:

1. **Computation of the RR intervals for each signal**
2. **Arrhythmic beat classification**
3. **Arrhythmic episode detection and classification**

4.1 RR Intervals Computation

The only feature extracted from the ECG is the R wave. The location of R waves is taken from the output of the beat detector algorithm described in chapter 3. The RR interval signal is constructed by measuring the time interval between successive R waves. Moreover, each computed RR is multiplied by a constant factor equal to 1.44 for adapting the values to the MIT-BIH database to adapt data to the MIT-BIH arrhythmia database.

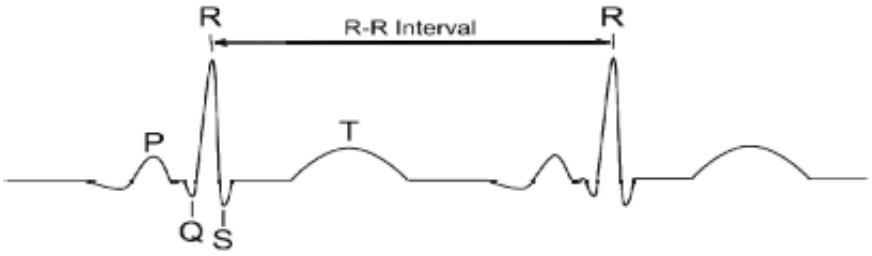

Figure 4.1. RR interval on a ECG trace

4.2 Arrhythmic Beat Classification

Arrhythmia beat-by-beat classification is performed on the RR-interval signal using a set of rules that were provided by medical experts and are based on clinical procedures for detecting arrhythmic events from the RR intervals.
The method works on a window of three RR intervals, for a total of four R waves. The third R wave is the one that is classified by the method. Hence, the first two R waves and the last R wave of each signal are excluded from the classification.
The beats are classified into four categories:

1. Normal Sinus Beats (N)

2. Premature Ventricular Contraction (PVC)

3. Ventricular Flutter/Fibrillation (VF)

4. 2nd Heart Block (BII)

The beat classification categories and their corresponding annotations from the MIT-BIH arrhythmia database for each category are given below:

Table 4.1. Beat classification categories

MIT-BIH Annotation Symbol	Type of Arrhythmia	Classification
N	Normal Beat	Normal (N)
P	Paced Beat	
f	Fusion of paced and normal beat	
P	Non-conducted P wave (blocked APB)	
L	Left bundle branch block beat	
R	Right bundle branch block beat	
Q	Unclassifiable Beat	
V	Premature Ventricular Contraction	Premature Ventricular Contraction (PVC)
[	Start of Ventricular flutter/fibrillation	Ventricular Flutter/Fibrillation (VF)
!	Ventricular flutter wave	
]	End of Ventricular flutter/fibrillation	
(BII	2nd Heart block	2nd Heart block (BII)

It is assumed that a beat not belonging to one of the arrhythmic categories indicated in the table is classified as normal.
The algorithm starts with a window i of three RR intervals, that are indicated as $RR1_i$, $RR2_i$ and $RR3_i$. The middle RR-interval is considered a priori normal and is classified in category 1.
Three rules are applied in this method :

- **Rule 1:** The rule is based on the classification of the total VF episode and not the classification of a single beat. Therefore, it is triggered if $RR2_i$ is much smaller than $RR1_i$ ($RR1_i > 1.8 \cdot RR2_i$) and the duration of $RR2_i$ is less than 0.6s. In this case, $RR2_i$ is considered as the start of a Ventricular Fibrillation (VF) episode and the next windows, from $i+1$ to n, are examined for two conditions.
  The first condition examines if the duration of all intervals in a window is less than 0.7s ($RR1_k < 0.7$ and $RR2_k < 0.7$ and $RR3_k < 0.7$) ensuring that all RR-intervals in the VF episode have a high frequency.
  The second condition controls if the total window duration is less than 1.7s ($RR1_k + RR2_k + RR3_k < 1.7$). This condition ensures that if one of the RR-interval does not have a duration less than 0.7s, but the total window duration is small, then it is considered as a continuing VF episode and not as two separate episodes.
  If only one of these two conditions is verified, then the middle interval is classified in category 3. When a window is reached, where none of the two conditions is true, then the VF episode has ended. Note that, if the number of consecutive VF classifications is less than 4, the algorithm returns to window i and continues with the next rule since there is a threshold of four consecutive

classified RR-intervals to define a VF episode.

- **Rule 2:** For what concern Premature Ventricular Contraction (PVC) classification, we have three conditions. If one of these three conditions is true then the $RR2_i$ is classified as PVC.

  - Condition 1: If $RR1_i > 1.15 \cdot RR2_i$ and $RR3_i > 1.15 \cdot RR2_i$ then isolated PVCs are classified

  - Condition 2: If $|RR1_i - RR2_i| < 0.3s$ and both $RR1_i$ and $RR2_i$ intervals are less than 0.8s and $RR3_i > 1.2 \cdot mean(RR1_i, RR2_i)$. Then the PVC couplets are classified. This is because the first two intervals of the window i must be short and of approximately the same length and the last interval of the window i must be longer than the other two.

  - Condition 3: If $|RR2_i - RR3_i|$ is less than 0.3s and both $RR2_i$ and $RR3_i$ intervals are less than 0.8s and $RR1_i > 1.2 \cdot mean(RR2_i, RR3_i)$ then PVC couplets are classified.This is because the last two intervals of the window i must be short and of approximately the same length and the first interval of the window i must be longer than the other two.

- **Rule 3:** In order to classify a BII beat we need two conditions. If both conditions are true, then the $RR2_i$ interval is classified as BII.

  - Condition 1: It checks if the duration of the $RR2_i$ is more than 2.2s and less than 3s ($2.2 < RR2_i < 3.0$).

  - Condition 2: This conditions controls if $|RR1_i - RR2_i|$ is less than 0.2s or $|RR2_i - RR3_i|$ is less than 0.2s. This condition ensures that an RR-interval, which satisfies condition 1, is not isolated and is almost equal to the previous or the next RR-interval.

The algorithm goes on with all the windows applying these rules sequentially and if a beat is classified to a category by one rule then this classification cannot be changed by one of the following rules.

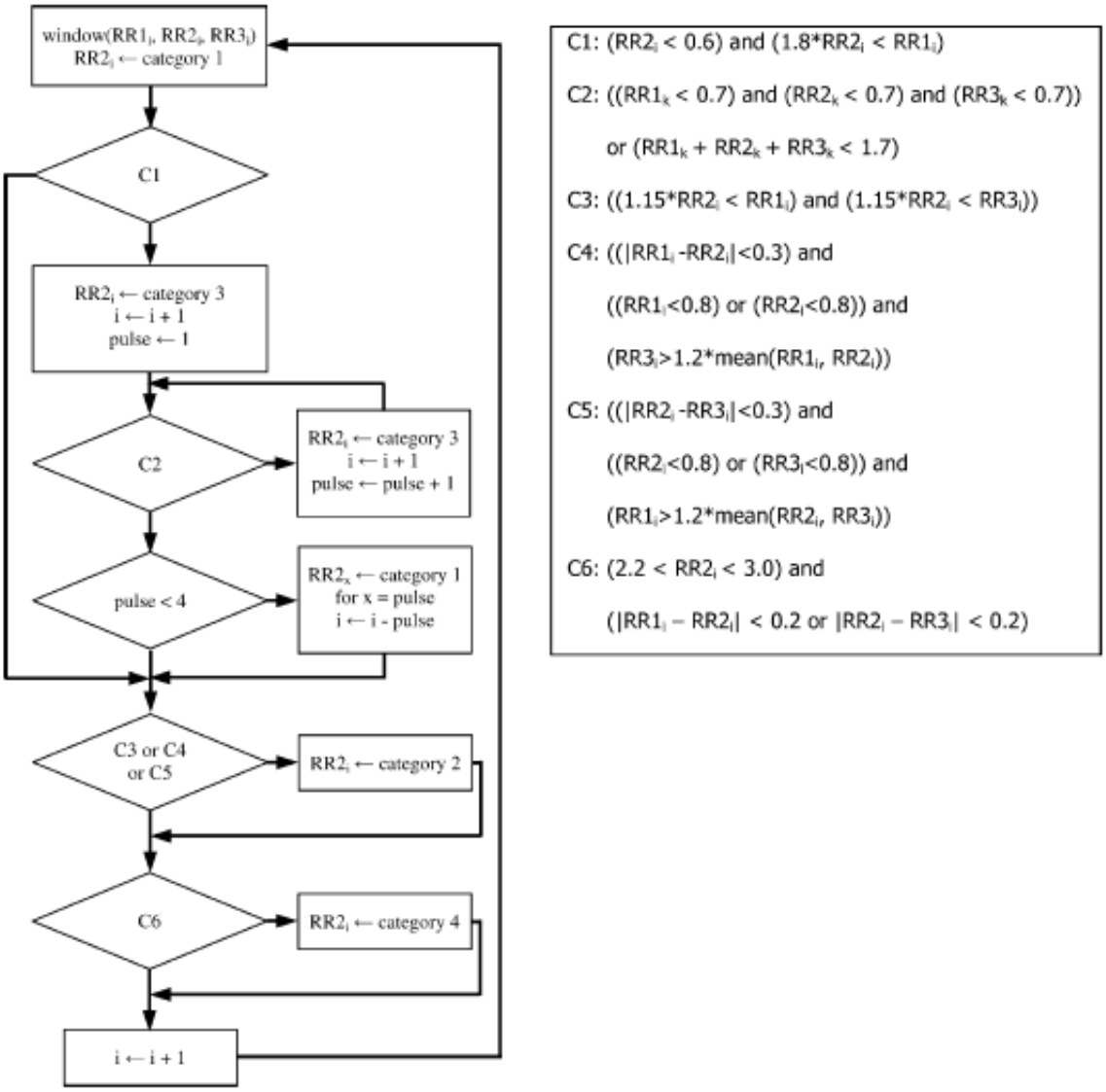

Figure 4.2. Diagram of the beat classification algorithm

4.3 Arrhythmic Episode Detection and Classification

Arrhythmic episode detection and classification is performed using the deterministic automaton represented below:

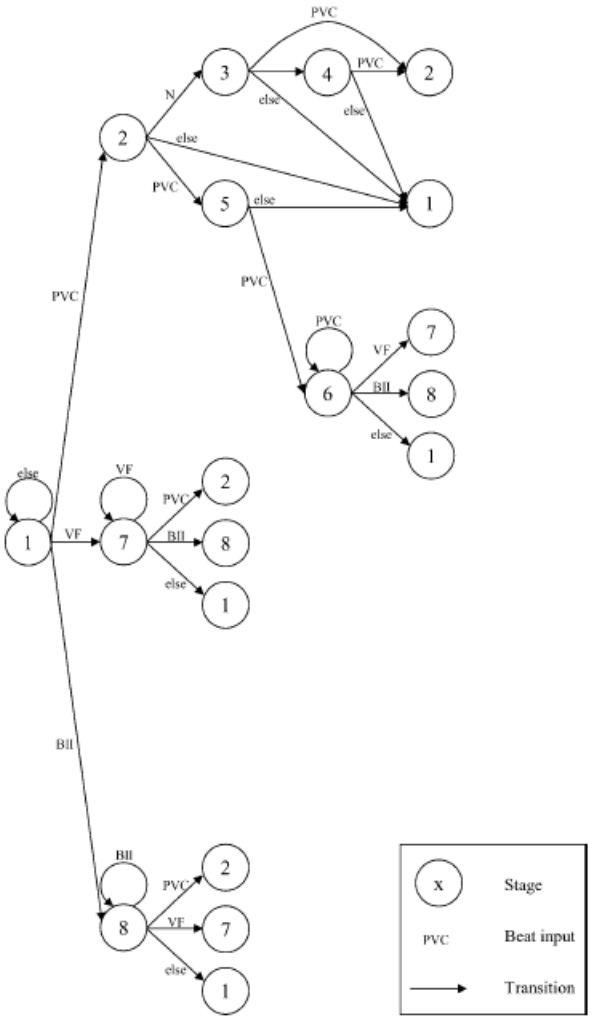

Figure 4.3. Deterministic automaton used for arrhythmic episode detection and classification

Six types of arrhythmic episodes can be detected and classified:

1. **Ventricular Bigeminy:** It requires at least 5 beats to be classified (PVC - N - PVC - N - PVC)

2. **Ventricular Trigeminy:** It requires at least 7 beats to be classified (PVC - N - N - PVC - N - N - PVC)

3. **Ventricular Couplet:** It requires 2 consequent PVCs to be classified

4. **Ventricular Tachycardia:** It requires at least 3 consequent PVCs to be classified

5. **Ventricular Flutter/Fibrillation:** It requires at least 3 consequent VFs to be classified

6. **2nd Heart Block:** It requires at least 2 consequent BIIs to be classified.

It is assumed that the rhythm is normal unless an episode belonging to one of the above arrhythmia types is detected and classified.
All episodes start with a specified type of classified beat and end with any type of classified beat. (e.g. a ventricular flutter/fibrillation episode is considered as a sequence of beats: VF - VF - ...- VF - XX, where XX is any type of beat other than VF).
The algorithm is divided into 8 different stages, each of which is described in detail below:

- **Stage 1:** Initial stage of the automaton. If a PVC, VF or BII classified beat occurs then the automaton proceeds to the appropriate stage (stages 2, 7 or 8); otherwise it remains in stage 1

- **Stage 2:** Possible ventricular bigeminy, trigeminy, couplet or tachycardia. If the next beat is N then the automaton proceeds to stage 3. If the next beat is a PVC and a bigeminy or trigeminy episode has already started, the beat is considered as the end of the episode and the automaton proceeds to stage 5. If the next beat is neither N nor a PVC and a bigeminy or trigeminy episode has already started, the beat is considered as the end of the episode and the automaton returns to stage 1.

- **Stage 3:** Possible ventricular bigeminy. If the next beat is a PVC and a trigeminy episode has already started, the beat is considered as the end of the episode and the automaton returns to stage 2. If the next beat is N and a bigeminy episode has already started, the beat is considered as the end of the episode and the automaton returns to stage 1, otherwise it proceeds to stage 4. If the next beat is neither N nor a PVC and a bigeminy or a trigeminy episode has already started, the beat is considered as the end of the episode and the automaton returns to stage 1

- **Stage 4:** Possible ventricular trigeminy. If the next beat is a PVC then the automaton returns to stage 2; otherwise, if a trigeminy episode has already started, the beat is considered as the end of the episode and the automaton returns to stage 1

- **Stage 5:** Ventricular couplet or tachycardia. The beat sequence is PVC-PVC so if the next beat is a PVC then the automaton proceeds to stage 6 for ventricular tachycardia (three consecutive PVC beats), otherwise it recognizes a ventricular couplet and returns to stage 1

- **Stage 6:** Ventricular tachycardia. Three consecutive PVC classified beats have been recognized, so a ventricular tachycardia episode is detected. However, the number of beats in the episode must be determined. Therefore, as long as PVC beats are recognized the automaton remains at stage 8. The first non-PVC classified beat will determine the end of the episode and the stage to which the automaton will proceed (stage 7 if classified as a VF, stage 8 if classified as a BII and stage 1 if classified otherwise)

- **Stage 7:** Ventricular flutter/fibrillation. A VF classified beat occurred and is considered as the start of a ventricular flutter/fibrillation episode. The number of beats in the episode must be determined and as long as VF beats follow the automaton remains at stage 7. The first non-VF classified beat will determine the end of the episode and the stage to which the automaton will proceed (stage 2 if classified as a PVC, stage 8 if classified as a BII and stage 1 if classified otherwise)

- **Stage 8:** 2nd heart block. A BII classified beat occurred and is considered as the start of a heart block episode. The number of beats in the episode must be determined, therefore as long as BII beats are recognized the automaton remains at stage 8. The first non-BII classified beat will determine the end of the episode and the stage to which the automaton will proceed (stage 2 if classified as a PVC, stage 7 if classified as a VF and stage 1 if classified otherwise)

An arrhythmic episode is identified only when a minimum number of beats has been reached. For ventricular bigeminy (PVC-N-PVC-N-PVC) this number is 5 beats, for ventricular trigeminy is 7 beats (PVC-N-N-PVC-N-N-PVC), for ventricular tachycardia is 3 beats (PVC-PVC-PVC), for ventricular fibrillation again 3 beats (VF-VF-VF) and for second heart block two beats are needed (BII-BII).
A very important rule of this algorithm is that if more than one rhythm type occurs the one that started first prevails (e.g. in the PVC-PVC-N-PVC-N-PVC sequence a ventricular couplet is detected and not a ventricular bigeminy episode or both a couplet and a bigeminy).

4.4 Results

As we described in section 4.2, we labeled each QRS complex into four beat categories:

1. **Normal**
2. **Premature Ventricular Contraction**
3. **Ventricular Fibrillation**
4. **Second Degree Heart Block**

In the following, we can see two confusion matrices, where each category has an ID, respectively :

- **Premature Ventricular Contraction:** 0
- **Ventricular Fibrillation:** 1
- **Normal:** 2
- **Second Degree Heart Block:** 3

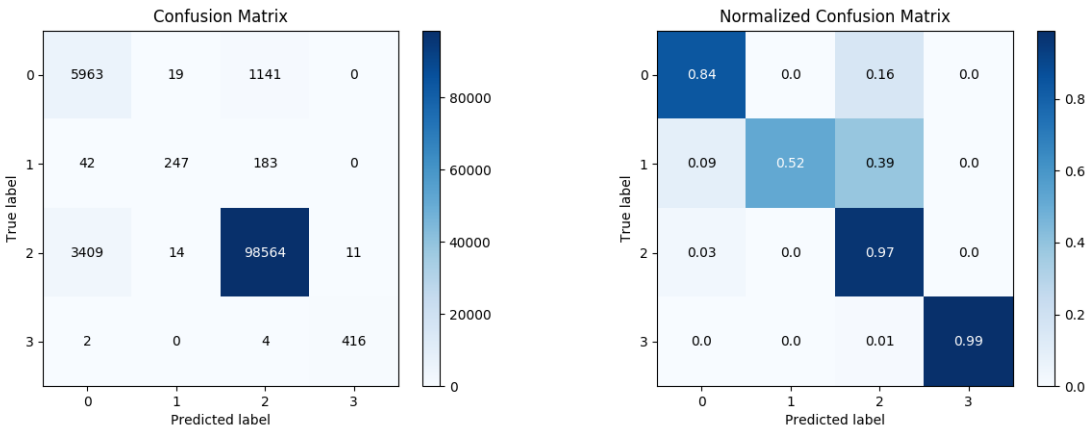

We can easily see that the best classified categories are the ones representing Normal beats with 97% and 2nd degree heart block with 99%, that are respectively the most and less populated classes. PVCs are still classified with a good score, precisely 84%, while the VFs beats are the ones with less precision with a score of 52%. Ventricular fibrillation has such a low precision given that around 40% of the total ventricular fibrillation beats are misclassified as normal beats. Also PVCs are often misclassified as normal beats but that is more common since a PVC differ from a normal beat just for its enhanced width and height.
Once we got the classified beats, we applied the arrhythmia detection and classification algorithm described in section 4.3. Results are shown below.

Table 4.2. Results comparison between dataset labeled episodes and detected episodes

Arrhythmia episode	Total Existing Episodes	Total Detected Episodes
Ventricular Couplets	813	470
Ventricular Bigeminy	221	446
Ventricular Trigeminy	83	0
Ventricular Tachycardia	71	47
Ventricular flutter/fibrillation	6	10
2nd Heart block	5	8

As we can see from the table, ventricular couplets is the most populated class of arrhythmia episodes both in the real world and in the algorithm's results as well. However, we detected only the 58% of the episodes. This problem is due to the missing of some PVCs in the previous step of the algorithm given that, as we described in **??**, a ventricular couplet is formed by two consecutive PVCs and missing one of them means missing the whole episode. Moreover, a relevant data that can be extracted from the results is that the algorithm did not detected a single ventricular trigeminy episode but detected twice the real ventricular bigeminy episodes, that means these two episodes are often misclassified since they are similar, (PVC-N-N-PVC-N-N-PVC for trigeminy and PVC-N-PVC-N-PVC for bigeminy). For what concern ventricular fibrillation and 2nd degree heart block, in the real world they are present only in two patients, respectively VF in the patient 207 (6 episodes) and 2nd heart block in the patient 231 (5 episodes). The algorithm reaches the 100% score in detecting episodes for these two patients but it wrongly classifies 4 VFs and 3 second degree heart block on other patients.

Once again, we decided to run the algorithm on all the machines we applied beat detection algorithms to, that are described in section 3.6 and the results are shown in the table below.

	Intel(R) Core (TM) i3-3240 CPU @3.40GHz, 4 cores	Arm Cortex-A53 CPU @2.1GHz, 4 cores	Arm Cortex-A53 CPU @2.1GHz, 4 cores @1.7GHz, 4 cores	Qualcomm Snapdragon 600 CPU @1.9 GHz, 4 cores
Single Beat Classification	0.0561	0.00036	0.00019	0.000482
Arrhythmic Episode Detection	0.0004	0.00420	0.00273	0.002558

However, as we can see from the picture below, the algorithm achieves good score in classifying each beat between two simpler categories such as :

- **Normal beats**

- **Abnormal beats**

In this alternative evaluation, the algorithm achieves 83% accuracy in classifying abnormal beats and 97% accuracy in classifying normal beats, that is a good score for what concern beat classification and could be useful to medical experts to analyze deeper abnormal beats.

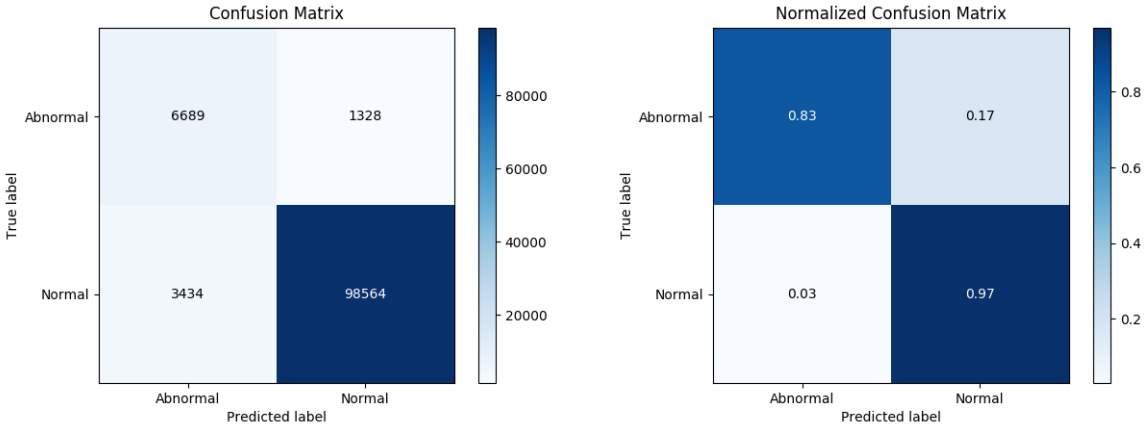

Chapter 5

Conclusion and Future works

We have implemented a real-time QRS detection algorithm in Python, starting from a Matlab code, in order to let it be runnable on mobile devices such as android devices. This algorithm reliably detects QRS complexes using slope, amplitude, and width information. A bandpass filter preprocesses the signal to reduce interference, permitting the use of low amplitude thresholds in order to get high detection sensitivity. In the algorithm, we used a dual-thresholds technique and search-back for missed beats. The algorithm periodically adapts each threshold and RR interval limit automatically. This adaptive approach provides for accurate use on ECG signals having many diverse signal characteristics, QRS morphologies, and heart rate changes. We took into account the MIT-BIH Arrhythmia Database for performance evaluation and the algorithm achieves a precision and recall score of 98.4%
Moreover, we implemented a method for arrhythmia beat classification and arrhythmic episode detection and classification. The method is based on the RR-interval signal extracted from ECG recordings. Hence, this approach is limited to detecting types of arrhythmic episodes that are related to the information carried by the RR-interval signal. Thus, arrhythmias such as atrial flutter and atrial fibrillation cannot be detected. Expert cardiologists have proposed the range of the values of the parameters used in this work and a set of rules was created. This set of rules is used for classifying beats in four beat categories and a deterministic automaton is used for detecting arrhythmic episode and for classifying them into six categories. Both, the rules and the deterministic automaton, are based on medical knowledge and observations upon RR-intervals of arrhythmic episodes. The method is advantageous to what is present in the literature because it uses a single feature, that is the RR-interval signal, which can be extracted with high accuracy even for noisy or complicated ECG recordings. This leads to a reduced processing time since only one feature is required compared to other methods that use more features or other types of ECG analysis. Moreover, it is based on medical knowledge, that is usually ignored in similar systems.
Again, the evaluation of the method was performed using the MIT-BIH arrhythmia database achieving a good score for what concern beat classification. In this algorithm, we focused on ventricular arrhythmias, since it only relies on RR intervals, but an alternative approach would be that of recognizing cardiac rhythms (premature beat, bigeminy, trigeminy, tachycardia, fibrillation) differentiating them between

atrial and ventricular origin of the arrhythmia, using new ECG features (such as the P waves) to accomplish this differentiation. Since the method performs in real time and is not affected by noise and alterations in arrhythmic episodes, it can be proven very useful in clinical practice.

Bibliography

[1] Eduardo JosÃĺ da S. Luz, William Robson Schwartz, Guillermo CÃąmara-ChÃąvez, David Menotti *ECG-based heartbeat classification for arrhythmia detection: A survey* Computer Methods and Programs in Biomedicine (127(2016) 144-164), Elsevier

[2] Bert-Uwe Kohler, Carsten Hennig, Reinhold Orglmeister *The principles of Software QRS Detection* IEEE Engineering in Medicine and Biology. 2002

[3] Y. Wang, C. J. Deepu and Y. Lian *A computationally efficient QRS detection algorithm for wearable ECG sensors* Conf. Rec. 2011 Annu. Int. Conf. Engineering in Medicine and Biology Society

[4] F. Zhang, et al. *QRS Detection Based on Multi-Scale Mathematical Morphology for Wearable ECG Device in Body Area Networks* IEEE Trans. on Biomedical-Circuits and Systems, Vol.3, No.4, pp.220-228, Aug. 2009.

[5] Chieh-Li Chen and Chun-Te Chuang *A QRS Detection and R Point Recognition Method for Wearable Single-Lead ECG Devices* Sensors 2017

[6] Yande Xiang, Zhitao Lin and Jianyi Meng *Automatic QRS complex detection using two-level convolutional neural network* BioMed Central

[7] Marko Sarlija, Fran Jurisic and Sinisa Popovic *A Convolutional Neural Network Based Approach to QRS Detection* 10th International Symposium on Image and Signal Processing and Analysis (ISPA 2017)

[8] Douglas A. Coast and Gerald G. Cano *QRS detection based on Hidden Markov Modeling* IEEE ENGINEERING IN MEDICINE & BIOLOGY SOCIETY 11th ANNUAL INTERNATIONAL CONFERENCE CH2770-6/89/0000-0034

[9] Arzeno NM, Poon CS and Deng ZD *Quantitative analysis of QRS detection algorithms based on the first derivative of the ECG* Conf Proc IEEE Eng Med Biol Soc. 2006;1:1788-91

[10] Jinkwon Kim, Hangsik Shin *Simple and Robust Realtime QRS Detection Algorithm Based on Spatiotemporal Characteristic of the QRS Complex* Randall Lee Rasmusson, University at Buffalo, UNITED STATES. 2016.

[11] Xu X. and Liu Y. *Adaptive threshold for QRS complex detection based on wavelet transform* 27th Annual Int. Conf Proc IEEE Eng Med Biol Soc. 2005;7:7281-4

[12] Jiapu Pan and Willis J. Tompkins *A Real Time QRS Detection Algorithm* IEE Transactions on Biomedical Engineering, VOL. BME-32, NO.3, March 1985

[13] *Peak Utils Documentation* https://media.readthedocs.org/pdf/peakutils/latest/peakutils.pdf

[14] M.G. Tsipouras, D.I. Fotiadis, D. Sideris, Arrhythmia *classification using the RR-interval duration signal* Comput. Cardiol., 2002, pp. 485-488.

[15] *ST segment* https://lifeinthefastlane.com/ecg-st-segment-evaluation

[16] Ivaylo I Christov *Real time electrocardiogram QRS detection using combined adaptive threshold* BioMedical Engineering OnLine 2004

[17] Sandoe E, Sigurd B. *Arrhythmia: a guide to clinical Electrocardiology* Bingen: Publishing Partners Verlags GmbH, 1991.

[18] Association for the Advancement of Medical Instrumentation *Testing and reporting performance results of cardiac rhythm and ST segment measurement algorithms* American National Standard 2013 ,ANSI/AAMI EC57:2012

[19] S.-W. Chen, P.M. Clarkson, Q. Fan *A robust sequential detection algorithm for cardiac arrhythmia classification* IEEE Trans. Biomed. Eng. 43 (11) (1996) 1120-1124.

[20] R.G. Kumar, Y.S. Kumaraswamy *Investigation and classification of ECG beat using input output additional weighted feed forward neural network* InternationalConference on Signal Processing, Image Processing &Pattern Recognition (ICSIPR), 2013, pp. 200-205.

[21] H. Chen, B.-C. Cheng, G.-T. Liao, T.-C. Kuo *Hybrid classification engine for cardiac arrhythmia cloud service in elderly healthcare management* J. Vis. Lang. Comput. 25(6) (2014) 745-753.

[22] I. Christov, G. Bortolan *Ranking of pattern recognition parameters for premature ventricular contractions classification by neural networks* Phisyol. Meas. 25 (5)(2004) 1281-1290.

[23] S. Osowski, T.H. Linh *ECG beat recognition using fuzzy hybrid neural network* IEEE Trans. Biomed. Eng. 48 (11)(2001) 1265-1271.

[24] Periyasamy M. Mariappan, Dhanasekaran R. Raghavan, Shady H.E. Abdel Aleem, and Ahmed F. Zobaa *Effects of electromagnetic interference on the functional usage of medical equipment by 2G/3G/4G cellular phones* Areview. Journal of Advanced Research 7, 5 (2016), 727-738.

[25] Orestis Akrivopoulos, Dimitrios Amaxilatis, Athanasios Antoniou and Ioannis Chatzigiannakis *Design and Evaluation of a Person-Centric Heart Monitoring System over Fog Computing Infrastructure* 2017 Association for Computing Machinery

[26] C. Tselios and G. Tsolis *On QoE-awareness through Virtualized Probes in 5G Networks Computer Aided Modeling and Design of Communication Links and Networks* (CAMAD), 2016 IEEE 21st International Workshop on, 2016, pp. 1-5

[27] M. Chiang and T. Zhang *Fog and Iot: An overview of research opportunities* IEEE Internet of Things Journal, vol. 3, no. 6, pp. 854-864, Dec 2016

[28] Orestis Akrivopoulos, Ioannis Chatzigiannakis, Christos Tselios and Athanasios Antoniou *On the Deployment of Healthcare Applications over Fog Computing Infrastructure*

[29] Van G.V., Podmasteryev K.V. *Algorithm for detection the QRS complexes based on support vector machine Scientific-Educational Center of "Biomedical engineering"* Orel State University named after I.S.Turgenev, 29 Naugorskoe sh., Orel, 302020, Russia

[30] Indu Saini, Dilbag Singh, Arun Khosla *QRS detection using K-Nearest Neighbor algorithm (KNN) and evaluation on standard ECG databases* Cairo University Journal of Advanced Research

[31] Ieong Chio In, Wan Feng, Vai Mang I, Mak Peng Un *QRS complex detector using Artificial Neural Network* University of Macau Macau, China, Faculty of Science and Technology

[32] RauÌĄl Alonso AÌĄlvarez, Arturo J. MeÌĄndez PeniÌĄn, X. AntoÌĄn Vila Sobrino *A comparison of three QRS detection algorithms over a public database* CENTERIS, 2013

[33] Portet F, Hernandez AI, Carrault G. *Evaluation of real-time QRS detection algorithms in variable contexts* Medical and Biological Engineering and Computing 2005

[34] Gail Walraven *Basic Arrhythmias* Brady 7th Edition

[35] George B. Moody and Roger G. Mark *The impact of the MIT-BIH Arrhythmia Database* IEEE ENGINEERING IN MEDICINE AND BIOLOGY 2001

[36] Dale Dubin *Rapid Interpretation of EKG's* 6th Edition

[37] B. Lown, M.D. Klein, P.I. Hershberg *Coronary and precoronary care* Amer. J. Med. 46 (1969) 705-724.

[38] M. Kundu, M. Nasipuri, D.K. Basu *Knowledge-based ECG interpretation: a critical review* 2000 Pattern Recognition Society

[39] Hooman Sedghamiz *Matlab implementation of Pan Tompkins ECG QRS Detector* March, 2014